

MONOTONE FINITE DIFFERENCE DOMAIN DECOMPOSITION ALGORITHMS AND APPLICATIONS TO NONLINEAR SINGULARLY PERTURBED REACTION-DIFFUSION PROBLEMS

IGOR BOGLAEV AND MATTHEW HARDY

Received 16 September 2004; Revised 21 December 2004; Accepted 11 January 2005

This paper deals with monotone finite difference iterative algorithms for solving nonlinear singularly perturbed reaction-diffusion problems of elliptic and parabolic types. Monotone domain decomposition algorithms based on a Schwarz alternating method and on box-domain decomposition are constructed. These monotone algorithms solve only linear discrete systems at each iterative step and converge monotonically to the exact solution of the nonlinear discrete problems. The rate of convergence of the monotone domain decomposition algorithms are estimated. Numerical experiments are presented.

Copyright © 2006 Hindawi Publishing Corporation. All rights reserved.

1. Introduction

We are interested in monotone discrete Schwarz alternating algorithms for solving nonlinear singularly perturbed reaction-diffusion problems.

The first problem considered corresponds to the singularly perturbed reaction-diffusion problem of elliptic type

$$\begin{aligned} -\mu^2(u_{xx} + u_{yy}) + f(x, y, u) &= 0, & (x, y) \in \omega, \\ u &= g \quad \text{on } \partial\omega, & \omega = \omega^x \times \omega^y = \{0 < x < 1\} \times \{0 < y < 1\}, \\ f_u &\geq c_*, & (x, y, u) \in \bar{\omega} \times (-\infty, \infty), & f_u \equiv \partial f / \partial u, \end{aligned} \quad (1.1)$$

where μ is a small positive parameter, $c_* > 0$ is a constant, $\partial\omega$ is the boundary of ω . If f and g are sufficiently smooth, then under suitable continuity and compatibility conditions on the data, a unique solution u of (1.1) exists (see [6] for details). Furthermore, for $\mu \ll 1$, problem (1.1) is singularly perturbed and characterized by boundary layers (i.e., regions with rapid change of the solution) of width $O(\mu |\ln \mu|)$ near $\partial\omega$ (see [1] for details).

2 Monotone domain decomposition algorithms

The second problem considered corresponds to the singularly perturbed reaction-diffusion problem of parabolic type

$$\begin{aligned} -\mu^2(u_{xx} + u_{yy}) + f(x, y, t, u) + u_t &= 0, & (x, y) \in \omega, t \in (0, T], \\ f_u &\geq 0, & (x, y, t, u) \in \bar{\omega} \times [0, T] \times (-\infty, \infty), \end{aligned} \quad (1.2)$$

where $\omega = \{0 < x < 1\} \times \{0 < y < 1\}$ and μ is a small positive parameter. The initial-boundary conditions are defined by

$$\begin{aligned} u(x, y, 0) &= u^0(x, y), & (x, y) \in \bar{\omega}, \\ u(x, y, t) &= g(x, y, t), & (x, y, t) \in \partial\omega \times (0, T]. \end{aligned} \quad (1.3)$$

The functions f , g , and u^0 are sufficiently smooth. Under suitable continuity and compatibility conditions on the data, a unique solution u of (1.2) exists (see [5] for details). For $\mu \ll 1$, problem (1.2) is singularly perturbed and characterized by the boundary layers of width $O(\mu|\ln\mu|)$ at the boundary $\partial\omega$ (see [2] for details). We mention that the assumption $f_u \geq 0$ in (1.2) can always be obtained via a change of variables.

In solving such nonlinear singularly perturbed problems by the finite difference method, the corresponding discrete problem is usually formulated as a system of nonlinear algebraic equations. One then requires a reliable and efficient computational algorithm for computing the solution. A fruitful method for the treatment of these nonlinear systems is the method of upper and lower solutions and its associated monotone iterations (in the case of unperturbed problems with reaction-diffusion equations see [8, 9] and the references therein). Since the initial iteration in the monotone iterative method is either an upper or lower solution constructed directly from the difference equations without any knowledge of the exact solution (see [3, 4] for details), this method eliminates the search for the initial iteration as is often needed in Newton's method. This gives a practical advantage in the computation of numerical solutions.

Iterative domain decomposition algorithms based on Schwarz-type alternating procedures have received much attention for their potential as efficient algorithms for parallel computing. In [3, 4], for solving the nonlinear problems (1.1) and (1.2), respectively, we proposed discrete iterative algorithms which combine the monotone approach and an iterative domain decomposition method based on the Schwarz alternating procedure. The spatial computational domain is partitioned into many nonoverlapping subdomains (vertical strips) with interface γ . Small interfacial subdomains are introduced near the interface γ , and approximate boundary values computed on γ are used for solving problems on nonoverlapping subdomains. Thus, this approach may be considered as a variant of a block Gauss-Seidel iteration (or in the parallel context as a multicoloured algorithm) for the subdomains with a Dirichlet-Dirichlet coupling through the interface variables. In this paper, we generalize the monotone domain decomposition algorithms from [3, 4] and employ a box-domain decomposition of the spatial computational domain. This leads to vertical and horizontal interfaces γ and ρ , and corresponding vertical and horizontal interfacial subdomain problems provide Dirichlet data on γ and ρ for the problems on the nonoverlapping box-subdomains.

In Section 2, we introduce the classical nonlinear finite difference schemes for the numerical solution of (1.1) and (1.2). Iterative methods by which each of these schemes may be solved are presented in [3, 4]. From an arbitrary initial mesh function, one may construct a sequence of functions which converges monotonically to the exact solution of the nonlinear difference scheme. Each function in the sequence is generated as the solution of a linear difference problem. In Section 3, we consider the elliptic problem and extend the monotone method to a box-decomposition of the computational domain. We show that monotonic convergence is maintained under the proposed decomposition and associated algorithm. Further, we develop estimates of the rate of convergence. The box-decomposition of the spatial domain is applied to the parabolic nonlinear difference scheme in Section 4. Numerical experiments are presented in Section 5. These confirm the theoretical estimates of the earlier sections. Suggestions are made regarding future parallel implementation.

2. Difference schemes for solving (1.1) and (1.2)

On $\bar{\omega}$ and $[0, T]$ introduce nonuniform meshes $\bar{\omega}^h = \bar{\omega}^{hx} \times \bar{\omega}^{hy}$ and $\bar{\omega}^\tau$:

$$\begin{aligned}\bar{\omega}^{hx} &= \{x_i, 0 \leq i \leq N_x; x_0 = 0, x_{N_x} = 1; h_{xi} = x_{i+1} - x_i\}, \\ \bar{\omega}^{hy} &= \{y_j, 0 \leq j \leq N_y; y_0 = 0, y_{N_y} = 1; h_{yj} = y_{j+1} - y_j\}, \\ \bar{\omega}^\tau &= \{t_k = k\tau, 0 \leq k \leq N_\tau, N_\tau \tau = T\}.\end{aligned}\tag{2.1}$$

For approximation of the elliptic problem (1.1), we use the classical difference scheme on nonuniform meshes

$$\mathcal{L}^h U + f(P, U) = 0, \quad P \in \omega^h, \quad U = g \text{ on } \partial\omega^h,\tag{2.2}$$

where $\mathcal{L}^h U$ is defined by

$$\mathcal{L}^h U = -\mu^2 (\mathcal{D}_x^2 + \mathcal{D}_y^2) U,\tag{2.3}$$

and $\mathcal{D}_x^2 U(P)$, $\mathcal{D}_y^2 U(P)$ are the central difference approximations to the second derivatives

$$\begin{aligned}\mathcal{D}_x^2 U_{ij} &= (\hbar_{xi})^{-1} \left[(U_{i+1,j} - U_{ij})(h_{xi})^{-1} - (U_{ij} - U_{i-1,j})(h_{x,i-1})^{-1} \right], \\ \mathcal{D}_y^2 U_{ij} &= (\hbar_{yj})^{-1} \left[(U_{i,j+1} - U_{ij})(h_{yj})^{-1} - (U_{ij} - U_{i,j-1})(h_{y,j-1})^{-1} \right], \\ \hbar_{xi} &= 2^{-1}(h_{x,i-1} + h_{xi}), \quad \hbar_{yj} = 2^{-1}(h_{y,j-1} + h_{yj}),\end{aligned}\tag{2.4}$$

where $P = (x_i, y_j) \in \bar{\omega}^h$ and $U_{ij} = U(x_i, y_j)$.

4 Monotone domain decomposition algorithms

To approximate the parabolic problem (1.2), we use the implicit difference scheme

$$\begin{aligned} \mathcal{L}^{h\tau}U(P,t) + f(P,t,U) &= \tau^{-1}U(P,t-\tau), \quad (P,t) \in \omega^h \times \omega^\tau, \\ \mathcal{L}^{h\tau}U(P,t) &\equiv \mathcal{L}^hU(P,t) + \tau^{-1}U(P,t), \\ U(P,0) &= u^0(P), \quad P \in \bar{\omega}^h, \quad U(P,t) = g(P,t), \quad (P,t) \in \partial\omega^h \times \omega^\tau, \end{aligned} \quad (2.5)$$

where \mathcal{L}^h is defined in (2.3).

Consider the linear versions of problems (2.2) and (2.5)

$$\begin{aligned} \mathcal{L}W + c(P)W(P) &= F(P), \quad P \in \omega^h, \\ W(P) &= W^0(P), \quad P \in \partial\omega^h, \quad c(P) \geq c_0 > 0, \quad P \in \bar{\omega}^h, \quad c_0 = \text{const}, \end{aligned} \quad (2.6)$$

where $\mathcal{L} = \mathcal{L}^h$ for (2.2) and $\mathcal{L} = \mathcal{L}^{h\tau}$ for (2.5). Now we formulate the maximum principle for the difference operator $\mathcal{L} + c$ and give an estimate of the solution to (2.6).

LEMMA 2.1. (i) *If $W(P)$ satisfies the conditions*

$$\mathcal{L}W + c(P)W(P) \geq 0 (\leq 0), \quad P \in \omega^h, \quad W(P) \geq 0 (\leq 0), \quad P \in \partial\omega^h, \quad (2.7)$$

then $W(P) \geq 0 (\leq 0)$, $P \in \bar{\omega}^h$.

(ii) *The following estimate of the solution to (2.6) holds true*

$$\begin{aligned} \|W\|_{\bar{\omega}^h} &\leq \max[\|W^0\|_{\partial\omega^h}, \|F\|_{\omega^h}/(c_0 + \beta\tau^{-1})], \\ \|W^0\|_{\partial\omega^h} &\equiv \max_{P \in \partial\omega^h} |W^0(P)|, \quad \|F\|_{\omega^h} \equiv \max_{P \in \omega^h} |F(P)|, \end{aligned} \quad (2.8)$$

where $\beta = 0$ for (2.2) and $\beta = 1$ for (2.5).

The proof of the lemma can be found in [11].

3. Monotone domain decomposition algorithm for the elliptic problem (1.1)

We consider a rectangular decomposition of the spatial domain $\bar{\omega}$ into $(M \times L)$ nonoverlapping subdomains $\bar{\omega}_{ml}$, $m = 1, \dots, M$, $l = 1, \dots, L$:

$$\omega_{ml} = (x_{m-1}, x_m) \times (y_{l-1}, y_l), \quad x_0 = 0, \quad x_M = 1, \quad y_0 = 0, \quad y_L = 1. \quad (3.1)$$

Additionally, we introduce $(M - 1)$ interfacial subdomains θ_m , $m = 1, \dots, M - 1$ (vertical strips):

$$\begin{aligned} \theta_m &= \theta_m^x \times \omega^y = \{x_m^b < x < x_m^e\} \times \{0 < y < 1\}, \quad \theta_{m-1} \cap \theta_m = \emptyset, \\ \gamma_m^b &= \{x = x_m^b, 0 \leq y \leq 1\}, \quad \gamma_m^e = \{x = x_m^e, 0 \leq y \leq 1\}, \\ x_m^b &< x_m < x_m^e, \quad \gamma_m^0 = \partial\omega \cap \partial\theta_m, \end{aligned} \quad (3.2)$$

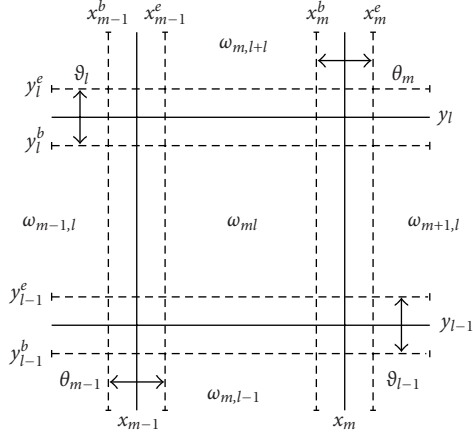


Figure 3.1. Fragment of the domain decomposition.

and $(L - 1)$ interfacial subdomains $\vartheta_l, l = 1, \dots, L - 1$ (horizontal strips):

$$\begin{aligned} \vartheta_l &= \omega^x \times \vartheta_l^y = \{0 < x < 1\} \times \{y_l^b < y < y_l^e\}, \quad \vartheta_{l-1} \cap \vartheta_l = \emptyset, \\ \rho_l^b &= \{0 \leq x \leq 1, y = y_l^b\}, \quad \rho_l^e = \{0 \leq x \leq 1, y = y_l^e\}, \\ y_l^b &< y_l < y_l^e, \quad \rho_l^0 = \partial\omega \cap \partial\vartheta_l. \end{aligned} \quad (3.3)$$

Figure 3.1 illustrates a fragment of the domain decomposition.

On $\bar{\omega}_{ml}, m = 1, \dots, M, l = 1, \dots, L; \bar{\theta}_m, m = 1, \dots, M - 1$ and $\bar{\vartheta}_l, l = 1, \dots, L - 1$, introduce meshes:

$$\begin{aligned} \bar{\omega}_{ml}^h &= \bar{\omega}_{ml} \cap \bar{\omega}^h, \quad \bar{\theta}_m^h = \bar{\theta}_m \cap \bar{\omega}^h, \quad \bar{\vartheta}_l^h = \bar{\vartheta}_l \cap \bar{\omega}^h, \\ \{x_m^b, x_m, x_m^e\}_{m=1}^{M-1} &\in \omega^{hx}, \quad \{y_l^b, y_l, y_l^e\}_{l=1}^{L-1} \in \omega^{hy}, \end{aligned} \quad (3.4)$$

with $\bar{\omega}^{hx}, \bar{\omega}^{hy}$ from (2.1).

3.1. Statement of domain decomposition algorithm. We consider the following domain decomposition approach for solving (2.2). On each iterative step, we first solve problems on the nonoverlapping subdomains $\bar{\omega}_{ml}^h, m = 1, \dots, M, l = 1, \dots, L$ with Dirichlet boundary conditions passed from the previous iterate. Then Dirichlet data are passed from these subdomains to the vertical and horizontal interfacial subdomains $\bar{\theta}_m^h, m = 1, \dots, M - 1$ and $\bar{\vartheta}_l^h, l = 1, \dots, L - 1$, respectively. Problems on the vertical interfacial subdomains are computed. Then Dirichlet data from these subdomains are passed to the horizontal interfacial subdomains before the corresponding linear problems are solved. Finally, we piece together the solutions on the subdomains.

Step 1. Initialization: On the whole mesh $\bar{\omega}^h$, choose an initial mesh function $V^{(0)}(P), P \in \bar{\omega}^h$ satisfying the boundary conditions $V^{(0)}(P) = g(P)$ on $\partial\omega^h$.

6 Monotone domain decomposition algorithms

Step 2. On subdomains $\bar{\omega}_{ml}^h$, $m = 1, \dots, M$, $l = 1, \dots, L$, compute mesh functions $V_{ml}^{(n+1)}(P)$ (here the index n stands for a number of iterative steps) satisfying the following difference problems

$$\begin{aligned} (\mathcal{L}^h + c^*)Z_{ml}^{(n+1)} &= -G^{(n)}(P), \quad P \in \omega_{ml}^h, \\ G^{(n)}(P) &\equiv \mathcal{L}^h V^{(n)} + f(P, V^{(n)}), \quad Z_{ml}^{(n+1)}(P) = 0, \quad P \in \partial\omega_{ml}^h, \\ V_{ml}^{(n+1)}(P) &= V^{(n)}(P) + Z_{ml}^{(n+1)}(P), \quad P \in \bar{\omega}_{ml}^h. \end{aligned} \quad (3.5)$$

Step 3. On the vertical interfacial subdomains $\bar{\theta}_m^h$, $m = 1, \dots, M-1$, compute the difference problems

$$\begin{aligned} (\mathcal{L}^h + c^*)Z_m^{(n+1)} &= -G^{(n)}(P), \quad P \in \theta_m^h, \\ Z_m^{(n+1)}(P) &= \begin{cases} 0, & P \in \gamma_m^{h0}; \\ Z_{ml}^{(n+1)}(P), & P \in \gamma_m^{hb} \cap \bar{\omega}_{ml}^h, \quad l = 1, \dots, L; \\ Z_{m+1,l}^{(n+1)}(P), & P \in \gamma_m^{he} \cap \bar{\omega}_{m+1,l}^h, \quad l = 1, \dots, L, \end{cases} \\ V_m^{(n+1)}(P) &= V^{(n)}(P) + Z_m^{(n+1)}(P), \quad P \in \bar{\theta}_m^h, \end{aligned} \quad (3.6)$$

where we use the notation

$$\gamma_m^{h0} = \gamma_m^0 \cap \partial\omega^h, \quad \gamma_m^{hb} = \gamma_m^b \cap \bar{\theta}_m^h, \quad \gamma_m^{he} = \gamma_m^e \cap \bar{\theta}_m^h. \quad (3.7)$$

Step 4. On the horizontal interfacial subdomains $\bar{\vartheta}_l^h$, $l = 1, \dots, L-1$, compute the following difference problems

$$\begin{aligned} (\mathcal{L}^h + c^*)\tilde{Z}_l^{(n+1)} &= -G^{(n)}(P), \quad P \in \vartheta_l^h, \\ \tilde{Z}_l^{(n+1)}(P) &= \begin{cases} 0, & P \in \rho_l^{h0}; \\ Z_{ml}^{(n+1)}(P), & P \in (\rho_l^{hb} \setminus \theta^h) \cap \bar{\omega}_{ml}^h, \quad m = 1, \dots, M; \\ Z_{m,l+1}^{(n+1)}(P), & P \in (\rho_l^{he} \setminus \theta^h) \cap \bar{\omega}_{m,l+1}^h, \quad m = 1, \dots, M; \\ Z_m^{(n+1)}(P), & P \in \partial\vartheta_l^h \cap \theta_m^h, \quad m = 1, \dots, M-1, \end{cases} \\ \tilde{V}_l^{(n+1)}(P) &= V^{(n)}(P) + \tilde{Z}_l^{(n+1)}(P), \quad P \in \bar{\vartheta}_l^h, \end{aligned} \quad (3.8)$$

where we use the notation

$$\begin{aligned} \bar{\theta}^h &= \bigcup_{m=1}^{M-1} \bar{\theta}_m^h, & \bar{\vartheta}^h &= \bigcup_{l=1}^{L-1} \bar{\vartheta}_l^h, \\ \rho_l^{h0} &= \rho_l^0 \cap \partial\omega^h, & \rho_l^{hb} &= \rho_l^b \cap \bar{\vartheta}_l^h, & \rho_l^{he} &= \rho_l^e \cap \bar{\vartheta}_l^h. \end{aligned} \quad (3.9)$$

Step 5. Compute the mesh function $V^{(n+1)}(P)$, $P \in \bar{\omega}^h$ by piecing together the solutions on the subdomains

$$V^{(n+1)}(P) = \begin{cases} V_{ml}^{(n+1)}(P), & P \in \bar{\omega}_{ml}^h \setminus (\bar{\theta}^h \cup \bar{\vartheta}^h); \\ V_m^{(n+1)}(P), & P \in \bar{\theta}_m^h \setminus \bar{\vartheta}^h, \quad m = 1, \dots, M-1; \\ \tilde{V}_l^{(n+1)}(P), & P \in \bar{\vartheta}_l^h, \quad l = 1, \dots, L-1. \end{cases} \quad (3.10)$$

Step 6. Stopping criterion: If a prescribed accuracy is reached, then stop; otherwise go to Step 2.

Algorithm (3.5)–(3.10) can be carried out by parallel processing. Steps 2, 3, and 4 must be performed sequentially, but on each step, the independent subproblems may be assigned to different computational nodes.

Remark 3.1. We note that the original Schwarz alternating algorithm with overlapping subdomains is a purely sequential algorithm. To obtain parallelism, one needs a subdomain colouring strategy, so that a set of independent subproblems can be introduced. The modification of the Schwarz algorithm (3.5)–(3.10) can be considered as an additive Schwarz algorithm.

3.2. Monotone convergence of algorithm (3.5)–(3.10). Additionally, we assume that f from (1.1) satisfies the two-sided constraints

$$0 < c_* \leq f_u \leq c^*, \quad c_*, c^* = \text{const.} \quad (3.11)$$

We say that $\bar{V}(P)$ is an upper solution of (2.2) if it satisfies the inequalities

$$\mathcal{L}^h \bar{V} + f(P, \bar{V}) \geq 0, \quad P \in \omega^h, \quad \bar{V} \geq g \text{ on } \partial\omega^h. \quad (3.12)$$

Similarly, $\underline{V}(P)$ is called a lower solution if it satisfies the reversed inequalities. Upper and lower solutions satisfy the following inequality

$$\underline{V}(P) \leq \bar{V}(P), \quad P \in \bar{\omega}^h, \quad (3.13)$$

since by the definitions of lower and upper solutions and the mean-value theorem, for $\delta V = \bar{V} - \underline{V}$ we have

$$\begin{aligned} \mathcal{L}^h \delta V + f_u(P) \delta V(P) &\geq 0, \quad P \in \omega^h, \\ \delta V(P) &\geq 0, \quad P \in \partial\omega^h, \end{aligned} \quad (3.14)$$

where $f_u(P) \equiv f_u[P, \underline{V}(P) + \Theta(P)\delta V(P)]$, $0 < \Theta(P) < 1$. In view of the maximum principle in Lemma 2.1, we conclude (3.13).

The following convergence property of algorithm (3.5)–(3.10) holds true.

8 Monotone domain decomposition algorithms

THEOREM 3.2. *Let $\overline{V}^{(0)}$ and $\underline{V}^{(0)}$ be upper and lower solutions of (2.2), and let $f(x, y, u)$ satisfy (3.11). Then the upper sequence $\{\overline{V}^{(n)}\}$ generated by (3.5)–(3.10) converges monotonically from above to the unique solution U of (2.2), and the lower sequence $\{\underline{V}^{(n)}\}$ generated by (3.5)–(3.10) converges monotonically from below to U :*

$$\underline{V}^{(0)} \leq \underline{V}^{(n)} \leq \underline{V}^{(n+1)} \leq U \leq \overline{V}^{(n+1)} \leq \overline{V}^{(n)} \leq \overline{V}^{(0)}, \quad \text{in } \overline{\omega}^h. \quad (3.15)$$

Proof. We consider only the case of the upper sequence. Let $\overline{V}^{(n)}$ be an upper solution. Then by the maximum principle in Lemma 2.1, from (3.5) we conclude that

$$Z_{ml}^{(n+1)}(P) \leq 0, \quad P \in \overline{\omega}_{ml}^h, \quad m = 1, \dots, M, \quad l = 1, \dots, L. \quad (3.16)$$

Using the mean-value theorem and the equation for $Z_{ml}^{(n+1)}(P)$, we obtain the difference equation for $V_{ml}^{(n+1)}$

$$\begin{aligned} \mathcal{L}^h V_{ml}^{(n+1)} + f(P, V_{ml}^{(n+1)}) &= -(c^* - f_{u,ml}^{(n)}(P))Z_{ml}^{(n+1)}(P) \geq 0, \quad P \in \omega_{ml}^h, \\ f_{u,ml}^{(n)}(P) &\equiv f_u[P, \overline{V}^{(n)}(P) + \Theta_{ml}^{(n)}(P)Z_{ml}^{(n+1)}(P)], \quad 0 < \Theta_{ml}^{(n)}(P) < 1, \\ V_{ml}^{(n+1)}(P) &= \overline{V}^{(n)}(P), \quad P \in \partial\omega_{ml}^h, \end{aligned} \quad (3.17)$$

where nonnegativeness of the right-hand side of the difference equation follows from (3.11) and (3.16).

Taking into account (3.16) and $\overline{V}^{(n)}$ is an upper solution, by the maximum principle in Lemma 2.1, from (3.6) and (3.8) it follows that

$$\begin{aligned} Z_m^{(n+1)}(P) &\leq 0, \quad P \in \overline{\theta}_m^h, \quad m = 1, \dots, M-1, \\ \tilde{Z}_l^{(n+1)}(P) &\leq 0, \quad P \in \overline{\vartheta}_l^h, \quad l = 1, \dots, L-1. \end{aligned} \quad (3.18)$$

Similar to (3.17), we obtain the difference problems for $V_m^{(n+1)}$

$$\begin{aligned} \mathcal{L}^h V_m^{(n+1)} + f(P, V_m^{(n+1)}) &= -(c^* - f_{u,m}^{(n)}(P))Z_m^{(n+1)}(P) \geq 0, \quad P \in \theta_m^h, \\ V_m^{(n+1)}(P) &= \begin{cases} g(P), & P \in \gamma_m^{h0}; \\ V_{ml}^{(n+1)}(P), & P \in \gamma_m^{hb} \cap \overline{\omega}_{ml}^h, \quad l = 1, \dots, L; \\ V_{m+1,l}^{(n+1)}(P), & P \in \gamma_m^{he} \cap \overline{\omega}_{m+1,l}^h, \quad l = 1, \dots, L, \end{cases} \end{aligned} \quad (3.19)$$

and for $\tilde{V}_l^{(n+1)}$

$$\begin{aligned} \mathcal{L}^h \tilde{V}_l^{(n+1)} + f(P, \tilde{V}_l^{(n+1)}) &= -(c^* - f_{u,l}^{(n)}(P)) \tilde{Z}_l^{(n+1)}(P) \geq 0, \quad P \in \vartheta_l^h, \\ \tilde{V}_l^{(n+1)}(P) &= \begin{cases} g(P), & P \in \rho_l^{h0}; \\ V_{ml}^{(n+1)}(P), & P \in (\rho_l^{hb} \setminus \theta^h) \cap \bar{\omega}_{ml}^h, \quad m = 1, \dots, M; \\ V_{m,l+1}^{(n+1)}(P), & P \in (\rho_l^{he} \setminus \theta^h) \cap \bar{\omega}_{m,l+1}^h, \quad m = 1, \dots, M; \\ V_m^{(n+1)}(P), & P \in \partial \vartheta_l^h \cap \bar{\theta}_m^h, \quad m = 1, \dots, M-1, \end{cases} \end{aligned} \quad (3.20)$$

where nonnegativeness of the right-hand sides of the difference equations follows from (3.11) and (3.18). Now we verify that the mesh function $\bar{V}^{(n+1)}$ defined by (3.10) is an upper solution. From the boundary conditions for $V_{ml}^{(n+1)}$, $V_m^{(n+1)}$ and $\tilde{V}_l^{(n)}$, it follows that $\bar{V}^{(n+1)}$ satisfies the boundary condition in (2.2). Now from here, (3.17), (3.19), (3.20) and the definition of $\bar{V}^{(n+1)}$ in (3.10), we conclude that

$$\begin{aligned} G^{(n+1)}(P) &= \mathcal{L}^h \bar{V}^{(n+1)} + f(P, \bar{V}^{(n+1)}) \geq 0, \quad P \in \omega^h \setminus (\tilde{\gamma}^h \cup \rho^h), \\ \tilde{\gamma}_{ml}^{hb,e} &= \{x_i = x_m^{b,e}, y_{l-1}^e < y_j < y_l^b\}, \quad \tilde{\gamma}_m^{hb,e} = \bigcup_{l=1}^L \tilde{\gamma}_{ml}^{hb,e}, \quad y_0^e = 0, \quad y_L^b = 1, \\ \tilde{\gamma}^h &= \bigcup_{m=1}^{M-1} \tilde{\gamma}_m^{hb,e}, \quad \rho^h = \bigcup_{l=1}^{L-1} \rho_l^{hb,e}. \end{aligned} \quad (3.21)$$

To prove that $\bar{V}^{(n+1)}$ is an upper solution of problem (2.2), we have to verify only that the last inequality holds true on the interfacial boundaries $\tilde{\gamma}_{ml}^{hb,e}$ and $\rho_l^{hb,e}$, $m = 1, \dots, M-1$, $l = 1, \dots, L-1$.

We check this inequality in the case of the left interfacial boundary $\tilde{\gamma}_{ml}^{hb}$, since the case with $\tilde{\gamma}_{ml}^{he}$ is checked in a similar way. From (3.5), (3.6), and (3.18), we conclude that the mesh function $W_{ml}^{(n+1)} = V_{ml}^{(n+1)} - V_m^{(n+1)}$ satisfies the difference problem

$$\begin{aligned} (\mathcal{L}^h + c^*) W_{ml}^{(n+1)} &= 0, \quad P \in \theta_{ml}^h = \omega_{ml}^h \cap \theta_m^h, \\ W_{ml}^{(n+1)}(P) &= \begin{cases} 0, & P \in \gamma_{ml}^{hb} = \gamma_m^{hb} \cap \bar{\omega}_{ml}^h; \\ \geq 0, & P \in \partial \theta_{ml}^h \setminus \gamma_{ml}^{hb}. \end{cases} \end{aligned} \quad (3.22)$$

In view of the maximum principle in Lemma 2.1,

$$V_{ml}^{(n+1)}(P) - V_m^{(n+1)}(P) \geq 0, \quad P \in \bar{\theta}_{ml}^h. \quad (3.23)$$

By (3.6), $V_m^{(n+1)}(P) = V_{ml}^{(n+1)}(P)$, $P \in \gamma_{ml}^{hb}$, and from (3.10) and (3.23), it follows that

$$\begin{aligned} -\mu^2 \mathcal{D}_y^2 V_{ml}^{(n+1)}(P) &= -\mu^2 \mathcal{D}_y^2 \bar{V}^{(n+1)}(P), \quad P \in \tilde{\gamma}_{ml}^{hb}, \\ -\mu^2 \mathcal{D}_x^2 V_{ml}^{(n+1)}(P) &\leq -\mu^2 \mathcal{D}_x^2 \bar{V}^{(n+1)}(P), \quad P \in \tilde{\gamma}_{ml}^{hb}. \end{aligned} \quad (3.24)$$

Thus, using (3.17), we conclude

$$G^{(n+1)}(P) \geq \mathcal{L}^h V_{ml}^{(n+1)}(P) + f(P, V_{ml}^{(n+1)}) \geq 0, \quad P \in \tilde{\mathcal{Y}}_{ml}^{hb}. \quad (3.25)$$

Now we verify the inequality $G^{(n+1)}(P) \geq 0$ on the interfacial boundary ρ_l^{hb} , and the case with ρ_l^{he} is checked in a similar way. From (3.5), (3.8), (3.18), and (3.23), we conclude that the mesh function $\tilde{W}_{ml}^{(n+1)} = V_{ml}^{(n+1)} - \tilde{V}_l^{(n+1)}$ satisfies the difference problem

$$\begin{aligned} (\mathcal{L}^h + c^*) \tilde{W}_{ml}^{(n+1)} &= 0, \quad P \in \mathfrak{g}_{ml}^h = \omega_{ml}^h \cap \mathfrak{g}_l^h, \\ \tilde{W}_{ml}^{(n+1)}(P) &= \begin{cases} 0, & P \in \tilde{\rho}_{ml}^{hb} = \{x_{m-1}^e < x_i < x_m^b, y_j = y_l^b\}; \\ \geq 0, & P \in \partial \mathfrak{g}_{ml}^h \setminus \tilde{\rho}_{ml}^{hb}. \end{cases} \end{aligned} \quad (3.26)$$

By the maximum principle in Lemma 2.1,

$$V_{ml}^{(n+1)}(P) - \tilde{V}_l^{(n+1)}(P) \geq 0, \quad P \in \bar{\mathfrak{g}}_{ml}^h. \quad (3.27)$$

By (3.8), $\tilde{V}_l^{(n+1)}(P) = V_{ml}^{(n+1)}(P)$, $P \in \tilde{\rho}_{ml}^{hb} \cup \{(x_{m-1}^e, y_l^b), (x_m^b, y_l^b)\}$, and from (3.10) and (3.27), it follows that

$$\begin{aligned} -\mu^2 \mathfrak{D}_x^2 V_{ml}^{(n+1)}(P) &= -\mu^2 \mathfrak{D}_x^2 \bar{V}^{(n+1)}(P), \quad P \in \tilde{\rho}_{ml}^{hb}, \\ -\mu^2 \mathfrak{D}_y^2 V_{ml}^{(n+1)}(P) &\leq -\mu^2 \mathfrak{D}_y^2 \bar{V}^{(n+1)}(P), \quad P \in \tilde{\rho}_{ml}^{hb}. \end{aligned} \quad (3.28)$$

Thus, using (3.17), we conclude

$$G^{(n+1)}(P) \geq \mathcal{L}^h V_{ml}^{(n+1)} + f(P, V_{ml}^{(n+1)}) \geq 0, \quad P \in \tilde{\rho}_{ml}^{hb}. \quad (3.29)$$

From (3.6), (3.8), and (3.27), the mesh function $\hat{W}_{ml}^{(n+1)} = V_m^{(n+1)} - \tilde{V}_l^{(n+1)}$ satisfies the difference problem

$$\begin{aligned} (\mathcal{L}^h + c^*) \hat{W}_{ml}^{(n+1)} &= 0, \quad P \in \tau_{ml}^h = \theta_m^h \cap \mathfrak{g}_l^h, \\ \hat{W}_{ml}^{(n+1)}(P) &= \begin{cases} 0, & P \in \hat{\rho}_{ml}^{hb,e} = \{x_m^b < x_i < x_m^e, y_j = y_l^{b,e}\}; \\ \geq 0, & P \in \partial \tau_{ml}^h \setminus (\hat{\rho}_{ml}^{hb} \cup \hat{\rho}_{ml}^{he}). \end{cases} \end{aligned} \quad (3.30)$$

By the maximum principle in Lemma 2.1,

$$V_m^{(n+1)}(P) - \tilde{V}_l^{(n+1)}(P) \geq 0, \quad P \in \bar{\tau}_{ml}^h. \quad (3.31)$$

By (3.8), $\tilde{V}_l^{(n+1)}(P) = V_m^{(n+1)}(P)$, $P \in \hat{\rho}_{ml}^{hb} \cup \{(x_m^e, y_l^b), (x_m^b, y_l^b)\}$, and from (3.10) and (3.31), it follows that

$$\begin{aligned} -\mu^2 \mathfrak{D}_x^2 V_m^{(n+1)}(P) &= -\mu^2 \mathfrak{D}_x^2 \bar{V}^{(n+1)}(P), \quad P \in \hat{\rho}_{ml}^{hb}, \\ -\mu^2 \mathfrak{D}_y^2 V_m^{(n+1)}(P) &\leq -\mu^2 \mathfrak{D}_y^2 \bar{V}^{(n+1)}(P), \quad P \in \hat{\rho}_{ml}^{hb}. \end{aligned} \quad (3.32)$$

Thus, using (3.19), we conclude

$$G^{(n+1)}(P) \geq \mathcal{L}^h V_m^{(n+1)} + f(P, V_m^{(n+1)}) \geq 0, \quad P \in \hat{\rho}_{ml}^{hb}. \quad (3.33)$$

From here and (3.29), we conclude the required inequality on $\rho_l^{hb} \setminus P_l^{b,e}, P_l^{b,e} = \cup_{m=1}^{M-1} (x_m^{b,e}, y_l^b)$. At $P_{ml}^b = (x_m^b, y_l^b)$, we have

$$V_{ml}^{(n+1)}(P_{ml}^b) = V_m^{(n+1)}(P_{ml}^b) = \tilde{V}_l^{(n+1)}(P_{ml}^b), \quad (3.34)$$

and from (3.10), it follows that

$$\begin{aligned} -\mu^2 \mathcal{D}_x^2 \bar{V}^{(n+1)}(P_{ml}^b) &= -\frac{\mu^2}{\tilde{h}_{xm}^b} \left[\frac{V_m^{(n+1)}(P_{ml}^{bx+}) - V_m^{(n+1)}(P_{ml}^b)}{\tilde{h}_{xm}^{b+}} - \frac{V_m^{(n+1)}(P_{ml}^b) - V_m^{(n+1)}(P_{ml}^{bx-})}{\tilde{h}_{xm}^{b-}} \right], \\ -\mu^2 \mathcal{D}_y^2 \bar{V}^{(n+1)}(P_{ml}^b) &= -\frac{\mu^2}{\tilde{h}_{yl}^b} \left[\frac{\tilde{V}_l^{(n+1)}(P_{ml}^{by+}) - V_m^{(n+1)}(P_{ml}^b)}{\tilde{h}_{yl}^{b+}} - \frac{V_m^{(n+1)}(P_{ml}^b) - V_m^{(n+1)}(P_{ml}^{by-})}{\tilde{h}_{yl}^{b-}} \right], \\ P_{ml}^{b\pm} &= (x_m^b \pm \tilde{h}_{xm}^{b\pm}, y_l^b), \quad P_{ml}^{by\pm} = (x_m^b, y_l^b \pm \tilde{h}_{yl}^{b\pm}), \\ \tilde{h}_{xm}^b &= 2^{-1}(\tilde{h}_{xm}^{b-} + \tilde{h}_{xm}^{b+}), \quad \tilde{h}_{yl}^b = 2^{-1}(\tilde{h}_{yl}^{b-} + \tilde{h}_{yl}^{b+}), \end{aligned} \quad (3.35)$$

where $\tilde{h}_{xm}^{b+}, \tilde{h}_{xm}^{b-}$ are the mesh step sizes on the left and right from P_{ml}^b , and $\tilde{h}_{yl}^{b+}, \tilde{h}_{yl}^{b-}$ are the mesh step sizes on the top and bottom from P_{ml}^b . From here, (3.17), (3.23) and (3.27), we conclude

$$G^{(n+1)}(P) \geq \mathcal{L}^h V_{ml}^{(n+1)} + f(P, V_{ml}^{(n+1)}) \geq 0, \quad P = P_{ml}^b. \quad (3.36)$$

With a similar argument for mesh point $P_l^e = (x_m^e, y_l^b)$, we prove that $\bar{V}^{(n+1)}$ is an upper solution of problem (2.2) on the whole computational domain $\bar{\omega}^h$.

For arbitrary $P \in \omega^h$, it follows from (3.16), (3.18), and (3.13) that the sequence $\{\bar{V}^{(n)}(P)\}$ is monotonically decreasing and bounded below by $\underline{V}(P)$, where \underline{V} is any lower solution. Therefore, the sequence is convergent and it follows from (3.5)–(3.8) that $\lim Z_{ml}^{(n)} = 0$, $\lim Z_l^{(n)} = 0$ and $\lim \tilde{Z}_l^{(n)} = 0$ as $n \rightarrow \infty$. Now by linearity of the operator \mathcal{L}^h and the continuity of f , we have also from (3.5)–(3.8) that the mesh function U defined by

$$U(P) = \lim_{n \rightarrow \infty} \bar{V}^{(n)}(P), \quad P \in \bar{\omega}^h, \quad (3.37)$$

is an exact solution to (2.2). The uniqueness of the solution to (2.2) follows from estimate (2.8). Indeed, if by contradiction, we assume that there exist two solutions U_1 and U_2 to (2.8), then by the mean-value theorem, the difference $\delta U = U_1 - U_2$ satisfies the following difference problem

$$\mathcal{L}^h \delta U + f_u \delta U = 0, \quad P \in \omega^h, \quad \delta U = 0, \quad P \in \partial \omega^h. \quad (3.38)$$

By (2.8), $\delta U = 0$ which leads to the uniqueness of the solution to (2.2). This proves the theorem. \square

Remark 3.3. Consider the following approach for constructing initial upper and lower solutions $\bar{V}^{(0)}$ and $\underline{V}^{(0)}$. Suppose that a mesh function $R(P)$ is defined on $\bar{\omega}^h$ and satisfies the boundary condition $R = g$ on $\partial\omega^h$. Introduce the following difference problems

$$\begin{aligned} (\mathcal{L}^h + c_*)Z_\nu^{(0)} &= \nu |\mathcal{L}^h R + f(P, R)|, \quad P \in \omega^h, \\ Z_\nu^{(0)}(P) &= 0, \quad P \in \partial\omega^h, \nu = 1, -1. \end{aligned} \quad (3.39)$$

Then the functions $\bar{V}^{(0)} = R + Z_1^{(0)}$, $\underline{V}^{(0)} = R + Z_{-1}^{(0)}$ are upper and lower solutions, respectively. The proof of this result can be found in [4].

Remark 3.4. Since the initial iteration in algorithm (3.5)–(3.10) is either an upper or a lower solution, which can be constructed directly from the difference equation without any knowledge of the solution as we have suggested in the previous remark, this algorithm eliminates the search for the initial iteration as is often needed in Newton's method. This gives a practical advantage in the computation of numerical solutions.

3.3. Convergence analysis of algorithm (3.5)–(3.10). We now establish convergence properties of algorithm (3.5)–(3.10).

If we denote

$$Z^{(n+1)}(P) = V^{(n+1)}(P) - V^{(n)}(P), \quad P \in \bar{\omega}^h, \quad (3.40)$$

then from (3.5)–(3.10), $Z^{(n+1)}$ can be written in the form

$$Z^{(n+1)}(P) = \begin{cases} Z_{ml}^{(n+1)}(P), & P \in \bar{\omega}_{ml}^h \setminus (\bar{\theta}^h \cup \bar{\vartheta}^h); \\ Z_m^{(n+1)}(P), & P \in \bar{\theta}_m^h \setminus \bar{\vartheta}^h, m = 1, \dots, M-1; \\ \tilde{Z}_l^{(n+1)}(P), & P \in \bar{\vartheta}_l^h, l = 1, \dots, L-1. \end{cases} \quad (3.41)$$

Introduce the following notation

$$\bar{h}_{xm}^{b,e} = 2^{-1}(h_{xm}^{b-,e-} + h_{xm}^{b+,e+}), \quad \bar{h}_{yl}^{b,e} = 2^{-1}(h_{yl}^{b-,e-} + h_{yl}^{b+,e+}), \quad (3.42)$$

where $h_{xm}^{b\pm, e\pm}$ are the mesh step sizes on the left and right from points $x_m^{b,e}$ and $h_{yl}^{b\pm, e\pm}$ are the mesh step sizes on the top and bottom from points $y_l^{b,e}$, and

$$\begin{aligned} \kappa_{xm}^b &\equiv \frac{\mu^2}{c^* \bar{h}_{xm}^b h_{xm}^{b+}}, & \kappa_{xm}^e &\equiv \frac{\mu^2}{c^* \bar{h}_{xm}^e h_{xm}^{e-}}, & q^I &= \max_{1 \leq m \leq M-1} \{\kappa_{xm}^b; \kappa_{xm}^e\}, \\ \kappa_{yl}^b &\equiv \frac{\mu^2}{c^* \bar{h}_{yl}^b h_{yl}^{b+}}, & \kappa_{yl}^e &\equiv \frac{\mu^2}{c^* \bar{h}_{yl}^e h_{yl}^{e-}}, & q^{II} &= \max_{1 \leq l \leq L-1} \{\kappa_{yl}^b; \kappa_{yl}^e\}. \end{aligned} \quad (3.43)$$

THEOREM 3.5. For algorithm (3.5)–(3.10), the following estimate holds true

$$\|Z^{(n+1)}\|_{\bar{\omega}^h} \leq \tilde{q} \|Z^{(n)}\|_{\bar{\omega}^h}, \quad \tilde{q} = q + (q^I + q^{II}), \quad (3.44)$$

where $q = 1 - c_*/c^*$.

Proof. Suppose that the sequence $\{V^{(n)}\}$ is generated by algorithm (3.5)–(3.10). Using (2.8), from (3.5) we get the following estimate on $Z_{ml}^{(n+1)}$

$$\|Z_{ml}^{(n+1)}\|_{\bar{\omega}_{ml}^h} \leq \frac{1}{c^*} \|G^{(n)}\|_{\omega^h}. \quad (3.45)$$

From here and (3.6) by (2.8), we conclude that

$$\begin{aligned} \|Z_m^{(n+1)}\|_{\bar{\theta}^h} &\leq \max \left\{ \frac{1}{c^*} \|G^{(n)}\|_{\omega^h}; \max_{1 \leq l \leq L} [\|Z_{ml}^{(n+1)}\|_{\gamma_{ml}^{hb}}; \|Z_{m+1,l}^{(n+1)}\|_{\gamma_{ml}^{he}}] \right\} \\ &\leq \frac{1}{c^*} \|G^{(n)}\|_{\omega^h}, \\ \gamma_{ml}^{hb} &= \gamma_m^{hb} \cap \bar{\omega}_{ml}^h, \quad \gamma_{ml}^{he} = \gamma_m^{he} \cap \bar{\omega}_{m+1,l}^h. \end{aligned} \quad (3.46)$$

Similarly, from here and (3.8), we can obtain the estimate

$$\|\tilde{Z}_l^{(n+1)}\|_{\bar{\theta}_l^h} \leq \frac{1}{c^*} \|G^{(n)}\|_{\omega^h}. \quad (3.47)$$

Thus, by the definition of $Z^{(n+1)}$, we have

$$\|Z^{(n+1)}\|_{\bar{\omega}^h} \leq \frac{1}{c^*} \|G^{(n)}\|_{\omega^h}. \quad (3.48)$$

From (3.17), (3.19) and (3.20) at the iterative step n , and using the definition of $Z^{(n)}$, we estimate $G^{(n)}$ as follows

$$G^{(n)}(P) = -(c^* - f_u^{(n)}(P))Z^{(n)}(P), \quad P \in \tilde{\omega}^h, \quad \tilde{\omega}^h = \omega^h \setminus (\tilde{\gamma}^h \cup \rho^h), \quad (3.49)$$

where $\tilde{\gamma}^h$ and ρ^h are defined in (3.21). By (3.11),

$$\frac{1}{c^*} \|G^{(n)}\|_{\tilde{\omega}^h} \leq q \|Z^{(n)}\|_{\bar{\omega}^h}. \quad (3.50)$$

Now we estimate $G^{(n)}$ on $\tilde{\gamma}^h$. On $\tilde{\gamma}_{ml}^{hb} = \{x_i = x_m^b, y_{i-1}^e < y_j < y_i^b\}$, we represent $G^{(n)}$ in the form

$$\begin{aligned} G^{(n)}(\tilde{P}_m^b) &= \mathcal{L}^h V_{ml}^{(n)} + f(\tilde{P}_m^b, V_{ml}^{(n)}) - \frac{\mu^2}{h_{xm}^b h_{xm}^{b+}} (V_m^{(n)}(\tilde{P}_m^{b+}) - V_{ml}^{(n)}(\tilde{P}_m^{b+})), \\ \tilde{P}_m^b &= (x_m^b, y_j) \in \tilde{\gamma}_{ml}^{hb}, \quad \tilde{P}_m^{b+} = (x_m^b + h_{xm}^{b+}, y_j). \end{aligned} \quad (3.51)$$

From (3.16) at the iterative step n and the definition of $V^{(n)}$, we have

$$V_{ml}^{(n)}(\tilde{P}_m^{b+}) - V_m^{(n)}(\tilde{P}_m^{b+}) \leq V_m^{(n-1)}(\tilde{P}_m^{b+}) - V_m^{(n)}(\tilde{P}_m^{b+}) = -Z^{(n)}(\tilde{P}_m^{b+}). \quad (3.52)$$

14 Monotone domain decomposition algorithms

From here, (3.17) and taking into account that $Z_{ml}^{(n)}(P) = Z^{(n)}(P)$, $P \in \tilde{\gamma}_{ml}^{hb}$, we get the estimate

$$\frac{1}{c^*} \|G^{(n)}\|_{\tilde{\gamma}_{ml}^{hb}} \leq (q + \kappa_{xm}^b) \|Z^{(n)}\|_{\bar{\omega}^h}. \quad (3.53)$$

Similarly, we can prove the estimate

$$\frac{1}{c^*} \|G^{(n)}\|_{\tilde{\gamma}_{ml}^{he}} \leq (q + \kappa_{xm}^e) \|Z^{(n)}\|_{\bar{\omega}^h}. \quad (3.54)$$

Thus, on $\tilde{\gamma}^h$, we conclude the estimate

$$\frac{1}{c^*} \|G^{(n)}\|_{\tilde{\gamma}^h} \leq (q + q^I) \|Z^{(n)}\|_{\bar{\omega}^h}. \quad (3.55)$$

On $\tilde{\rho}_{ml}^{hb} = \{x_{m-1}^e < x_i < x_m^b, y_j = y_l^b\}$, we represent $G^{(n)}$ in the form

$$\begin{aligned} G^{(n)}(P_l^b) &= \mathcal{L}^h V_{ml}^{(n)} + f(P_l^b, V_{ml}^{(n)}) - \frac{\mu^2}{\tilde{h}_{yl}^b h_{yl}^{b+}} (\tilde{V}_l^{(n)}(P_l^{b+}) - V_{ml}^{(n)}(P_l^{b+})), \\ P_l^b &= (x_i, y_l^b) \in \tilde{\rho}_{ml}^{hb}, \quad P_l^{b+} = (x_i, y_l^b + h_{yl}^{b+}). \end{aligned} \quad (3.56)$$

From (3.16) at the iterative step n and the definition of $V^{(n)}$, we have

$$V_{ml}^{(n)}(P_l^{b+}) - \tilde{V}_l^{(n)}(P_l^{b+}) \leq V^{(n-1)}(P_l^{b+}) - V^{(n)}(P_l^{b+}) = -Z^{(n)}(P_l^{b+}). \quad (3.57)$$

From here and (3.17), and taking into account that $Z_{ml}^{(n)}(P) = Z^{(n)}(P)$, $P \in \tilde{\rho}_{ml}^{hb}$, we get the estimate

$$\frac{1}{c^*} \|G^{(n)}\|_{\tilde{\rho}_{ml}^{hb}} \leq (q + \kappa_{yl}^b) \|Z^{(n)}\|_{\bar{\omega}^h}. \quad (3.58)$$

Similarly, we can prove the estimate

$$\frac{1}{c^*} \|G^{(n)}\|_{\tilde{\rho}_{ml}^{he}} \leq (q + \kappa_{yl}^e) \|Z^{(n)}\|_{\bar{\omega}^h}. \quad (3.59)$$

On $\hat{\rho}_{ml}^{hb} = \{x_m^b < x_i < x_m^e, y_j = y_l^b\}$, we represent $G^{(n)}$ in the form

$$\begin{aligned} G^{(n)}(P_l^b) &= \mathcal{L}^h V_m^{(n)} + f(P_l^b, V_m^{(n)}) - \frac{\mu^2}{\tilde{h}_{yl}^b h_{yl}^{b+}} (\tilde{V}_l^{(n)}(P_l^{b+}) - V_m^{(n)}(P_l^{b+})), \\ P_l^b &= (x_i, y_l^b) \in \hat{\rho}_{ml}^{hb}, \quad P_l^{b+} = (x_i, y_l^b + h_{yl}^{b+}). \end{aligned} \quad (3.60)$$

From (3.18) at the iterative step n and the definition of $V^{(n)}$, we have

$$V_m^{(n)}(P_l^{b+}) - \tilde{V}_l^{(n)}(P_l^{b+}) \leq V^{(n-1)}(P_l^{b+}) - V^{(n)}(P_l^{b+}) = -Z^{(n)}(P_l^{b+}). \quad (3.61)$$

From here and (3.19), and taking into account that $Z_m^{(n)}(P) = Z^{(n)}(P)$, $P \in \hat{\rho}_{ml}^{hb}$, we get the estimate

$$\frac{1}{c^*} \|G^{(n)}\|_{\hat{\rho}_{ml}^{hb}} \leq (q + \kappa_{yl}^b) \|Z^{(n)}\|_{\bar{\omega}^h}. \quad (3.62)$$

Similarly, we can prove the estimate

$$\frac{1}{c^*} \|G^{(n)}\|_{\hat{\rho}_{ml}^{he}} \leq (q + \kappa_{yl}^e) \|Z^{(n)}\|_{\bar{\omega}^h}. \quad (3.63)$$

At $P_{ml}^b = (x_m^b, y_l^b)$, we represent $G^{(n)}$ in the form

$$\begin{aligned} G^{(n)}(P_{ml}^b) &= \mathcal{L}^h V_{ml}^{(n)} + f(P_{ml}^b, V_{ml}^{(n)}) \\ &\quad - \frac{\mu^2}{\tilde{h}_{xm}^b h_{xm}^{b+}} (V_m^{(n)}(P_{ml}^{bx+}) - V_{ml}^{(n)}(P_{ml}^{bx+})) \\ &\quad - \frac{\mu^2}{\tilde{h}_{yl}^b h_{yl}^{b+}} (\tilde{V}_l^{(n)}(P_{ml}^{by+}) - V_{ml}^{(n)}(P_{ml}^{by+})), \end{aligned} \quad (3.64)$$

$$P_{ml}^{bx+} = (x_m^b + h_{xm}^{b+}, y_l^b), \quad P_{ml}^{by+} = (x_m^b, y_l^b + h_{yl}^{b+}).$$

From (3.16) at the iterative step n and the definition of $V^{(n)}$, we have

$$\begin{aligned} V_{ml}^{(n)}(P_{ml}^{bx+}) - V_m^{(n)}(P_{ml}^{bx+}) &\leq V^{(n-1)}(P_{ml}^{bx+}) - V^{(n)}(P_{ml}^{bx+}) \\ &= -Z^{(n)}(P_{ml}^{bx+}), \\ V_{ml}^{(n)}(P_{ml}^{by+}) - \tilde{V}_l^{(n)}(P_{ml}^{by+}) &\leq V^{(n-1)}(P_{ml}^{by+}) - V^{(n)}(P_{ml}^{by+}) \\ &= -Z^{(n)}(P_{ml}^{by+}). \end{aligned} \quad (3.65)$$

From here and (3.17), and taking into account that $Z_{ml}^{(n)}(P_{ml}^b) = Z^{(n)}(P_{ml}^b)$, we get the estimate

$$\frac{1}{c^*} |G^{(n)}(P_{ml}^b)| \leq (q + \kappa_{xm}^b + \kappa_{yl}^b) \|Z^{(n)}\|_{\bar{\omega}^h}. \quad (3.66)$$

By the same reasonings, the following estimate holds true

$$\frac{1}{c^*} |G^{(n)}(P_{m-1,l}^e)| \leq (q + \kappa_{x,m-1}^e + \kappa_{yl}^b) \|Z^{(n)}\|_{\bar{\omega}^h}, \quad P_{m-1,l}^e = (x_{m-1}^e, y_l^b). \quad (3.67)$$

On ρ_l^{hb} , we conclude the estimate

$$\frac{1}{c^*} \|G^{(n)}\|_{\rho_l^{hb}} \leq (q + q^I + q^{II}) \|Z^{(n)}\|_{\bar{\omega}^h}. \quad (3.68)$$

The same estimate holds true on ρ_l^{he} , and on ρ^h we get the estimate

$$\frac{1}{c^*} \|G^{(n)}\|_{\rho^h} \leq (q + q^I + q^{II}) \|Z^{(n)}\|_{\bar{\omega}^h}. \quad (3.69)$$

From here, (3.50) and (3.55), we conclude the estimate

$$\frac{1}{c_*} \|G^{(n)}\|_{\omega^h} \leq (q + q^I + q^{II}) \|Z^{(n)}\|_{\bar{\omega}^h}. \quad (3.70)$$

and, using (3.48), we prove the theorem. \square

Remark 3.6. For the undecomposed algorithm, with $M = 1$ and $L = 1$, one has $\tilde{\omega}^h = \omega^h$ in (3.50) which together with (3.48) gives estimate (3.44) with $\tilde{q} = q$.

Without loss of generality, we assume that the boundary condition in (1.1) is zero, that is, $g(P) = 0$. This assumption can always be obtained via a change of variables. Let the initial function $V^{(0)}$ be chosen in the form of (3.39) with $R(P) = 0$, that is, $V^{(0)}$ is the solution of the following difference problem

$$\begin{aligned} (\mathcal{L}^h + c_*) V^{(0)} &= \nu |f(P, 0)|, & P \in \omega^h, \\ V^{(0)}(P) &= 0, & P \in \partial\omega^h, & \nu = 1, -1. \end{aligned} \quad (3.71)$$

Then the functions $\bar{V}^{(0)}(P)$, $\underline{V}^{(0)}(P)$ corresponding to $\nu = 1$ and $\nu = -1$ are upper and lower solutions, respectively.

THEOREM 3.7. *Let the factor \tilde{q} in (3.44) satisfy the condition $\tilde{q} < 1$. Suppose that the initial upper or lower solution $V^{(0)}$ is chosen in the form of (3.71). Then for algorithm (3.5)–(3.10), the following estimate holds true*

$$\|V^{(n)} - U\|_{\bar{\omega}^h} \leq \frac{c_0(\tilde{q})^n}{(1 - \tilde{q})} \|f(P, 0)\|_{\bar{\omega}^h}, \quad c_0 = \frac{3c_* + c^*}{c_* c^*}, \quad (3.72)$$

where U is the solution to (2.2).

Proof. Using (3.44), we have

$$\begin{aligned} \|V^{(n+k)} - V^{(n)}\|_{\bar{\omega}^h} &\leq \sum_{i=n}^{n+k-1} \|V^{(i+1)} - V^{(i)}\|_{\bar{\omega}^h} = \sum_{i=n}^{n+k-1} \|Z^{(i+1)}\|_{\bar{\omega}^h} \\ &\leq \frac{\tilde{q}}{1 - \tilde{q}} \|Z^{(n)}\|_{\bar{\omega}^h} \leq \frac{(\tilde{q})^n}{1 - \tilde{q}} \|Z^{(1)}\|_{\bar{\omega}^h}. \end{aligned} \quad (3.73)$$

Taking into account that $\lim_{k \rightarrow \infty} V^{(n+k)} = U$ as $k \rightarrow \infty$, where U is the solution to (2.2), we conclude the estimate

$$\|V^{(n)} - U\|_{\bar{\omega}^h} \leq \frac{(\tilde{q})^n}{1 - \tilde{q}} \|Z^{(1)}\|_{\bar{\omega}^h}. \quad (3.74)$$

From (3.48), (3.71) and the mean-value theorem

$$\begin{aligned} \|Z^{(1)}\|_{\bar{\omega}^h} &\leq \frac{1}{c_*} \|G^{(0)}\|_{\omega^h} \leq \frac{1}{c_*} \|\mathcal{L}^h V^{(0)}\|_{\omega^h} + \frac{1}{c_*} \|f(P, V^{(0)})\|_{\bar{\omega}^h} \\ &\leq \frac{1}{c_*} (c_* \|V^{(0)}\|_{\bar{\omega}^h} + \|f(P, 0)\|_{\bar{\omega}^h}) + \frac{1}{c_*} \|f(P, 0)\|_{\bar{\omega}^h} + \|V^{(0)}\|_{\bar{\omega}^h}. \end{aligned} \quad (3.75)$$

From here and estimating $V^{(0)}$ from (3.71) with (2.8),

$$\|V^{(0)}\|_{\bar{\omega}^h} \leq \frac{1}{c_*} \|f(P, 0)\|_{\bar{\omega}^h}, \quad (3.76)$$

we conclude the estimate on $Z^{(1)}$ in the form

$$\|Z^{(1)}\|_{\bar{\omega}^h} \leq c_0 \|f(P, 0)\|_{\bar{\omega}^h}, \quad (3.77)$$

where c_0 is defined in (3.72). Thus, from here and (3.74), we prove (3.72). \square

Remark 3.8. In the next section, we present sufficient conditions to guarantee the inequality $\tilde{q} < 1$ required in Theorem 3.7.

3.4. Uniform convergence of the monotone domain decomposition algorithm (3.5)–(3.10). Here we analyze a convergence rate of algorithm (3.5)–(3.10) applied to the difference scheme (2.2) defined on the piecewise uniform mesh introduced in [7]. On this mesh, the difference scheme (2.2) converges μ -uniformly to the solution of (1.1).

The piecewise uniform mesh is formed in the following manner. We divide each of the intervals $\bar{\omega}^x = [0, 1]$ and $\bar{\omega}^y = [0, 1]$ into three parts each $[0, \sigma_x]$, $[\sigma_x, 1 - \sigma_x]$, $[1 - \sigma_x, 1]$, and $[0, \sigma_y]$, $[\sigma_y, 1 - \sigma_y]$, $[1 - \sigma_y, 1]$, respectively. Assuming that N_x, N_y are divisible by 4, in the parts $[0, \sigma_x]$, $[1 - \sigma_x, 1]$ and $[0, \sigma_y]$, $[1 - \sigma_y, 1]$ we use a uniform mesh with $N_x/4 + 1$ and $N_y/4 + 1$ mesh points, respectively, and in the parts $[\sigma_x, 1 - \sigma_x]$, $[\sigma_y, 1 - \sigma_y]$ with $N_x/2 + 1$ and $N_y/2 + 1$ mesh points, respectively. This defines the piecewise equidistant mesh in the x - and y -directions condensed in the boundary layers at $x = 0, 1$ and $y = 0, 1$:

$$x_i = \begin{cases} ih_{x\mu}, & i = 0, 1, \dots, N_x/4; \\ \sigma_x + (i - N_x/4)h_x, & i = N_x/4 + 1, \dots, 3N_x/4; \\ 1 - \sigma_x + (i - 3N_x/4)h_{x\mu}, & i = 3N_x/4 + 1, \dots, N_x, \end{cases} \quad (3.78)$$

$$y_j = \begin{cases} jh_{y\mu}, & j = 0, 1, \dots, N_y/4; \\ \sigma_y + (j - N_y/4)h_y, & j = N_y/4 + 1, \dots, 3N_y/4; \\ 1 - \sigma_y + (j - 3N_y/4)h_{y\mu}, & j = 3N_y/4 + 1, \dots, N_y, \end{cases}$$

where $h_{x\mu}, h_{y\mu}$ and h_x, h_y are the step sizes inside and outside the boundary layers, respectively. The transition points $\sigma_x, (1 - \sigma_x)$ and $\sigma_y, (1 - \sigma_y)$ are determined by

$$\sigma_x = \min \{4^{-1}, \mu c_*^{-1/2} \ln N_x\}, \quad \sigma_y = \min \{4^{-1}, \mu c_*^{-1/2} \ln N_y\}. \quad (3.79)$$

If $\sigma_{x,y} = 1/4$, then $N_{x,y}^{-1}$ are very small relative to μ . This is unlikely in practice, and in this case the difference scheme (2.2) can be analysed using standard techniques. We therefore

assume that

$$\begin{aligned}\sigma_x &= \mu c_*^{-(1/2)} \ln N_x, & h_{x\mu} &= 4\mu c_*^{-(1/2)} N_x^{-1} \ln N_x, & N_x^{-1} < h_x < 2N_x^{-1}, \\ \sigma_y &= \mu c_*^{-(1/2)} \ln N_y, & h_{y\mu} &= 4\mu c_*^{-(1/2)} N_y^{-1} \ln N_y, & N_y^{-1} < h_y < 2N_y^{-1}.\end{aligned}\quad (3.80)$$

The difference scheme (2.2) on the piecewise uniform mesh (3.80) converges μ -uniformly to the solution of (1.1):

$$\max_{P \in \bar{\omega}^h} |U(P) - u(P)| \leq C(N^{-1} \ln N)^2, \quad N = \min \{N_x, N_y\}, \quad (3.81)$$

where constant C is independent of μ and N . The proof of this result can be found in [7].

THEOREM 3.9. *Let the interfacial subdomains $\bar{\theta}_m^h$, $m = 1, \dots, M-1$ and $\bar{\vartheta}_l^h$, $l = 1, \dots, L-1$ be located in the x - and y -directions, respectively, outside the boundary layers. Assume $\mu \leq \mu_0 \ll 1$, and the following condition*

$$\bar{N} \leq \frac{\alpha \sqrt{c_*}/2}{\mu_0}, \quad \bar{N} = \max \{N_x, N_y\}, \quad 0 < \alpha < 1, \quad \alpha = \text{const.} \quad (3.82)$$

If the initial upper or lower solution $V^{(0)}$ is chosen in the form of (3.71), then the monotone domain decomposition algorithm (3.5)–(3.10) on the piecewise uniform mesh (3.80) converges μ -uniformly to the solution of the problem (1.1):

$$\begin{aligned}\|V^{(n)} - u\|_{\bar{\omega}^h} &\leq C(N^{-1} \ln N)^2 + \frac{c_0(\tilde{Q})^n}{(1 - \tilde{Q})} \|f(P, 0)\|_{\bar{\omega}^h}, \\ \tilde{Q} &= 1 - (1 - \alpha^2) \frac{c_*}{c^*} < 1, \quad c_0 = \frac{3c_* + c^*}{c_* c^*},\end{aligned}\quad (3.83)$$

where constant C and the factor \tilde{Q} are independent of μ and N .

Proof. Under the above assumption on \bar{N} , the factor \tilde{q} in (3.44) satisfies the condition $\tilde{q} < 1$. Indeed, since the interfacial subdomains are located outside the boundary layers, where the step sizes h_x and h_y are in use, then using (3.80), q^I and q^{II} from (3.44) are estimated as follows

$$q^I = \frac{\mu^2}{c^* h_x^2} < \frac{(\mu_0 \bar{N})^2}{c^*}, \quad q^{II} = \frac{\mu^2}{c^* h_y^2} < \frac{(\mu_0 \bar{N})^2}{c^*}. \quad (3.84)$$

Thus, $\tilde{q} < \tilde{Q} < 1$, and we can apply Theorem 3.7. From here, (3.72) and (3.81), we conclude the theorem. \square

Remark 3.10. Such domain decompositions, in which the interfacial subdomains are outside the boundary layers, are said to be *unbalanced*, since the distribution of mesh points among the nonoverlapping main subdomains is uneven. By contrast, a *balanced* domain decomposition is one in which the mesh points are equally distributed among the main subdomains. For balanced decompositions, the first and last interfacial subdomains each overlap the boundary layer.

4. Monotone domain decomposition algorithm for the parabolic problem (1.2)

For solving the nonlinear difference scheme (2.5), we construct and investigate a parallel domain decomposition algorithm based on the domain decomposition of the spatial domain $\bar{\omega}$ introduced in Section 3.

4.1. Statement of domain decomposition algorithm for solving (2.5). On each time level $t \in \omega^\tau$, we calculate n_* iterates $V^{(n)}(P, t)$, $P \in \bar{\omega}^h$, $n = 1, \dots, n_*$ as follows.

Step 1. Initialization: on the mesh $\bar{\omega}^h$, choose $V^{(0)}(P, t)$, $P \in \bar{\omega}^h$ satisfying the boundary condition $V^{(0)}(P, t) = g(P, t)$ on $\partial\omega^h$.

For $n = 0$ to $n_* - 1$ do Steps 2–5

Step 2. On subdomains $\bar{\omega}_{ml}^h$, $m = 1, \dots, M$, $l = 1, \dots, L$, compute mesh functions $V_{ml}^{(n+1)}(P, t)$, $m = 1, \dots, M$, $l = 1, \dots, L$ satisfying the following difference problems

$$\begin{aligned} (\mathcal{L}^{h\tau} + c^*)Z_{ml}^{(n+1)} &= -G^{(n)}(P, t), \quad P \in \omega_{ml}^h, \\ G^{(n)}(P, t) &\equiv \mathcal{L}^{h\tau} V^{(n)}(P, t) + f(P, t, V^{(n)}) - \tau^{-1} V(P, t - \tau), \\ Z_{ml}^{(n+1)}(P, t) &= 0, \quad P \in \partial\omega_{ml}^h, \\ V_{ml}^{(n+1)}(P, t) &= V^{(n)}(P, t) + Z_{ml}^{(n+1)}(P, t), \quad P \in \bar{\omega}_{ml}^h. \end{aligned} \tag{4.1}$$

Step 3. On the vertical interfacial subdomains $\bar{\theta}_m^h$, $m = 1, \dots, M - 1$, compute the difference problems

$$\begin{aligned} (\mathcal{L}^{h\tau} + c^*)Z_m^{(n+1)} &= -G^{(n)}(P, t), \quad P \in \theta_m^h, \\ Z_m^{(n+1)}(P, t) &= \begin{cases} 0, & P \in \gamma_m^{h0}; \\ Z_{ml}^{(n+1)}(P, t), & P \in \gamma_m^{hb} \cap \bar{\omega}_{ml}^h, \quad l = 1, \dots, L; \\ Z_{m+1,l}^{(n+1)}(P, t), & P \in \gamma_m^{he} \cap \bar{\omega}_{m+1,l}^h, \quad l = 1, \dots, L, \end{cases} \\ V_m^{(n+1)}(P, t) &= V^{(n)}(P, t) + Z_m^{(n+1)}(P, t), \quad P \in \bar{\theta}_m^h, \end{aligned} \tag{4.2}$$

where we use the notation from (3.6).

Step 4. On the horizontal interfacial subdomains $\bar{\mathfrak{D}}_l^h$, $l = 1, \dots, L-1$, compute the following difference problems

$$\begin{aligned}
 (\mathcal{L}^{hr} + c^*)\tilde{Z}_l^{(n+1)} &= -G^{(n)}(P, t), \quad P \in \mathfrak{D}_l^h, \\
 \tilde{Z}_l^{(n+1)}(P, t) &= \begin{cases} 0, & P \in \rho_l^{h0}; \\ Z_{ml}^{(n+1)}(P, t), & P \in (\rho_l^{hb} \setminus \theta^h) \cap \bar{\omega}_{ml}^h, \quad m = 1, \dots, M; \\ Z_{m,l+1}^{(n+1)}(P, t), & P \in (\rho_l^{he} \setminus \theta^h) \cap \bar{\omega}_{m,l+1}^h, \quad m = 1, \dots, M; \\ Z_m^{(n+1)}(P, t), & P \in \partial\mathfrak{D}_l^h \cap \theta_m^h, \quad m = 1, \dots, M-1, \end{cases} \\
 \tilde{V}_l^{(n+1)}(P, t) &= V^{(n)}(P, t) + \tilde{Z}_l^{(n+1)}(P, t), \quad P \in \bar{\mathfrak{D}}_l^h,
 \end{aligned} \tag{4.3}$$

where we use the notation from (3.8).

Step 5. Compute the mesh function $V^{(n+1)}(P, t)$, $P \in \bar{\omega}^h$ by piecing together the solutions on the subdomains

$$V^{(n+1)}(P, t) = \begin{cases} V_{ml}^{(n+1)}(P, t), & P \in \bar{\omega}_{ml}^h \setminus (\bar{\theta}^h \cup \bar{\mathfrak{D}}^h); \\ V_m^{(n+1)}(P, t), & P \in \bar{\theta}_m^h \setminus \bar{\mathfrak{D}}^h, \quad m = 1, \dots, M-1; \\ \tilde{V}_l^{(n+1)}(P, t), & P \in \bar{\mathfrak{D}}_l^h, \quad l = 1, \dots, L-1. \end{cases} \tag{4.4}$$

Step 6. Set up

$$V(P, t) = V^{(n_*)}(P, t), \quad P \in \bar{\omega}^h. \tag{4.5}$$

4.2. Monotone convergence of algorithm (4.1)–(4.5). Additionally, we assume that f from (1.2) satisfies the two-sided constraints

$$0 \leq f_u \leq c^*, \quad c^* = \text{const}. \tag{4.6}$$

On a time level $t \in \omega^\tau$, we say that $\bar{V}(P, t)$ is an upper solution with respect to a given function $V(P, t - \tau)$ if it satisfies

$$\begin{aligned}
 \mathcal{L}^{hr}\bar{V}(P, t) + f(P, t, \bar{V}) - \tau^{-1}V(P, t - \tau) &\geq 0, \quad P \in \omega^h, \\
 \bar{V}(P, t) &\geq g(P, t), \quad P \in \partial\omega^h.
 \end{aligned} \tag{4.7}$$

Similarly, $\underline{V}(P, t)$ is called a lower solution with respect to $V(P, t - \tau)$ if it satisfies the reversed inequalities. On each time level, upper and lower solutions satisfy the following inequality

$$\underline{V}(P, t) \leq \bar{V}(P, t), \quad P \in \bar{\omega}^h. \tag{4.8}$$

The proof of this result is similar to that of (3.13).

On each time level $t \in \omega^\tau$, we have the following convergence property of algorithm (4.1)–(4.5).

THEOREM 4.1. Let $V(P, t - \tau)$ be given and $\overline{V}^{(0)}(P, t)$, $\underline{V}^{(0)}(P, t)$ be upper and lower solutions corresponding to $V(P, t - \tau)$. Suppose that f satisfies (4.6). Then the upper sequence $\{\overline{V}^{(n)}(P, t)\}$ generated by (4.1)–(4.5) converges monotonically from above to the unique solution $\mathcal{V}(P, t)$ of the problem

$$\begin{aligned} \mathcal{L}^{hr} V(P, t) + f(P, t, V) - \tau^{-1} V(P, t - \tau) &= 0, & P \in \omega^h, \\ V(P, t) &= g(P, t), & P \in \partial\omega^h, \end{aligned} \quad (4.9)$$

and the lower sequence $\{\underline{V}^{(n)}(P, t)\}$ generated by (4.1)–(4.5) converges monotonically from below to $\mathcal{V}(P, t)$:

$$\begin{aligned} \mathcal{V}(P, t) &\leq \overline{V}^{(n+1)}(P, t) \leq \overline{V}^{(n)}(P, t) \leq \overline{V}^{(0)}(P, t), & P \in \overline{\omega}^h, \\ \underline{V}^{(0)}(P, t) &\leq \underline{V}^{(n)}(P, t) \leq \underline{V}^{(n+1)}(P, t) \leq \mathcal{V}(P, t), & P \in \overline{\omega}^h. \end{aligned} \quad (4.10)$$

Proof. The proof of the theorem is similar to the proof of Theorem 3.2 and based on the maximum principle in Lemma 2.1 and the estimate (2.8) with $\beta = 1$ for the difference operator \mathcal{L}^{hr} . \square

Remark 4.2. In the case of algorithm (4.1)–(4.5), Remarks 3.1–3.4 hold still true at each time step $t \in \omega^\tau$. We only mention that the difference problem in (3.39) becomes

$$\begin{aligned} \mathcal{L}^{hr} Z_\nu^{(0)} &= \nu | \mathcal{L}^{hr} R(P, t) + f(P, t, R) - \tau^{-1} V(P, t - \tau) |, & P \in \omega^h, \\ Z_\nu^{(0)}(P, t) &= 0, & P \in \partial\omega^h, \nu = 1, -1. \end{aligned} \quad (4.11)$$

4.3. Convergence analysis of algorithm (4.1)–(4.5). We now establish convergence properties of algorithm (4.1)–(4.5).

Introduce the following notation

$$\begin{aligned} v_{xm}^b &\equiv \frac{\mu^2}{(c^* + \tau^{-1}) h_{xm}^b h_{xm}^{b+}}, & v_{xm}^e &\equiv \frac{\mu^2}{(c^* + \tau^{-1}) h_{xm}^e h_{xm}^{e-}}, \\ v_{yl}^b &\equiv \frac{\mu^2}{(c^* + \tau^{-1}) h_{yl}^b h_{yl}^{b+}}, & v_{yl}^e &\equiv \frac{\mu^2}{(c^* + \tau^{-1}) h_{yl}^e h_{yl}^{e-}}, \\ r^I &= \max_{1 \leq m \leq M-1} \{v_{xm}^b; v_{xm}^e\}, & r^{II} &= \max_{1 \leq l \leq L-1} \{v_{yl}^b; v_{yl}^e\}, \end{aligned} \quad (4.12)$$

where all the step sizes are defined in (3.42).

Similar to Theorem 3.5, on each time level $t \in \omega^\tau$, we have the following convergence property of algorithm (4.1)–(4.5).

THEOREM 4.3. For algorithm (4.1)–(4.5), the following estimate holds true

$$\|Z^{(n+1)}(t)\|_{\overline{\omega}^h} \leq \tilde{r} \|Z^{(n)}(t)\|_{\overline{\omega}^h}, \quad \tilde{r} = r + (r^I + r^{II}), \quad t \in \omega^\tau, \quad (4.13)$$

where $Z^{(n)}(P, t) = V^{(n)}(P, t) - V^{(n-1)}(P, t)$ and $r = c^*/(c^* + \tau^{-1})$.

Proof. The proof of the theorem is similar to the proof of Theorem 3.5 and based on the maximum principle in Lemma 2.1 and the estimate (2.8) with $\beta = 1$ for the difference operator \mathcal{L}^{hr} . \square

Remark 4.4. In similar fashion to the proof of Theorem 3.5, the proof of Theorem 4.3 includes the result $\tilde{r} = r$ for the undecomposed algorithm.

Without loss of generality, we assume that for the parabolic problem (1.2), the boundary condition $g(P, t) = 0$. This assumption can always be obtained via a change of variables. Let on each time level the initial function $V^{(0)}(P, t)$ be chosen in the form of (4.11) with $R(P, t) = 0$, that is, $V^{(0)}(P, t)$ is the solution of the following difference problem

$$\begin{aligned} \mathcal{L}^{hr} V^{(0)}(P, t) &= \nu |f(P, t, 0) - \tau^{-1} V(P, t - \tau)|, \quad P \in \omega^h, \\ V^{(0)}(P, t) &= 0, \quad P \in \partial\omega^h, \quad \nu = 1, -1. \end{aligned} \tag{4.14}$$

Then the functions $\overline{V}^{(0)}(P, t)$, $\underline{V}^{(0)}(P, t)$ corresponding to $\nu = 1$ and $\nu = -1$ are upper and lower solutions, respectively.

THEOREM 4.5. *In the domain decomposition algorithm (4.1)–(4.5), let $V^{(0)}(P, t)$ be chosen in the form of (4.14), and let f satisfy (4.6). Suppose that on each time level, the number of iterates n_* satisfies $n_* \geq 2$. Then the following estimate on convergence rate holds*

$$\begin{aligned} \max_{t_k \in \omega^\tau} \|V(t_k) - U(t_k)\| &\leq D(c^* + \eta)(\tilde{r})^{n_* - 1}, \\ \eta &= (c^* + \tau^{-1})(r^I + r^{II}), \end{aligned} \tag{4.15}$$

where \tilde{r} , r^I and r^{II} are defined in Theorem 4.3, $U(P, t)$ is the solution to (2.5) and constant D is independent of μ and τ . Furthermore, on each time level the sequence $\{V^{(n)}(P, t)\}$ converges monotonically.

Proof. The difference problem for $V(P, t_k) = V^{(n_*)}(P, t_k)$ can be represented in the form

$$\begin{aligned} \mathcal{L}^{hr} V(P, t_k) + f(P, t_k, V) - \tau^{-1} V(P, t_{k-1}) &= G^{(n_*)}(P, t_k), \quad P \in \omega^h, \\ V(P, t_k) &= g(P, t_k), \quad P \in \partial\omega^h. \end{aligned} \tag{4.16}$$

From here, (2.5) and using the mean-value theorem, we get the difference problem for $W(P, t_k) = V(P, t_k) - U(P, t_k)$

$$\begin{aligned} (\mathcal{L}^{hr} + f_u^{(n_*)}) W(P, t_k) &= G^{(n_*)}(P, t_k) + \tau^{-1} W(P, t_{k-1}), \quad P \in \omega^h, \\ W(P, t_k) &= 0, \quad P \in \partial\omega^h. \end{aligned} \tag{4.17}$$

Using the same reasonings as in proving the estimate (3.70), we can obtain the following estimate on $G^{(n^*)}$:

$$\|G^{(n^*)}(t_k)\|_{\omega^h} \leq (c^* + \eta) \|Z^{(n^*)}(t_k)\|_{\bar{\omega}^h}. \quad (4.18)$$

By (2.8) and (4.13), we estimate the solution of (4.17) in the form

$$\|W(t_k)\|_{\bar{\omega}^h} \leq \tau(c^* + \eta) \tilde{r}^{n^*-1} \|Z^{(1)}(t_k)\|_{\bar{\omega}^h} + \|W(t_{k-1})\|_{\bar{\omega}^h}. \quad (4.19)$$

By (2.8), from (4.1)–(4.5), we have

$$\|Z^{(1)}(t_k)\|_{\bar{\omega}^h} \leq \tau \|\mathcal{L}^{h\tau} V^{(0)}(t_k) + f(V^{(0)}(t_k)) - \tau^{-1} V(t_{k-1})\|_{\omega^h}. \quad (4.20)$$

By the mean-value theorem,

$$f(P, t_k, V^{(0)}) = f(P, t_k, 0) + f_u^{(0)} V^{(0)}(P, t_k), \quad (4.21)$$

and from (4.20), it follows that

$$\|Z^{(1)}(t_k)\|_{\bar{\omega}^h} \leq \tau \|\mathcal{L}^{h\tau} V^{(0)}(t_k)\|_{\omega^h} + \tau \|f_u^{(0)} V^{(0)}(t_k)\|_{\bar{\omega}^h} + \tau \|f(P, t_k, 0) - \tau^{-1} V(t_{k-1})\|_{\bar{\omega}^h}. \quad (4.22)$$

From here, (4.14) and (4.6), and estimating $V^{(0)}$ from (4.14) by (2.8) with $\beta = 1$, we get

$$\begin{aligned} \|Z^{(1)}(t_k)\|_{\bar{\omega}^h} &\leq (2\tau + c^* \tau^2) \|f(P, t_k, 0) - \tau^{-1} V(t_{k-1})\|_{\bar{\omega}^h} \\ &\leq (2\tau + c^* \tau^2) (\|f(P, t_k, 0)\|_{\bar{\omega}^h} + \tau^{-1} \|V(t_{k-1})\|_{\bar{\omega}^h}) \leq D_k, \end{aligned} \quad (4.23)$$

where for sufficiently small τ , constant D_k is independent of τ . From here and (4.19), by induction we prove the estimate

$$\|W(t_k)\|_{\bar{\omega}^h} \leq \left(\sum_{l=1}^k D_l \right) \tau (c^* + \eta) (\tilde{r})^{n^*-1}, \quad k = 1, \dots, N_\tau. \quad (4.24)$$

Since $N_\tau \tau = T$, we prove the estimate (4.15) with $D = TD_0$, where $D_0 = \max_{1 \leq k \leq N_\tau} D_k$, and, hence, D is independent of τ .

To prove that all constants D_k are independent of the small parameter μ , we have to prove that $\|V(t_{k-1})\|_{\bar{\omega}^h}$ in (4.23) is μ -uniformly bounded. For $k = 1$, $V(P, 0) = u^0(P)$, where u^0 is the initial condition in the differential problem (1.2), and, hence, D_1 is independent of μ and τ . For $k = 2$, we have

$$\|Z^{(1)}(t_2)\|_{\bar{\omega}^h} \leq (2\tau + c^* \tau^2) \|f(P, t_2, 0)\|_{\bar{\omega}^h} + (2 + c^* \tau) \|V(t_1)\|_{\bar{\omega}^h} \leq D_2, \quad (4.25)$$

where $V(P, t_1) = V^{(n_*)}(P, t_1)$. As follows from Theorem 4.1, the monotone sequences $\{\overline{V}^{(n)}(P, t_1)\}$ and $\{\underline{V}^{(n)}(P, t_1)\}$ are μ -uniformly bounded from above by $\overline{V}^{(0)}(P, t_1)$ and from below by $\underline{V}^{(0)}(P, t_1)$. Applying (2.8) with $\beta = 1$ to the problem (4.14) at $t = t_1$, we have

$$\|V^{(0)}(t_1)\|_{\overline{\omega}^h} \leq \tau \|f(P, t_1, 0) - \tau^{-1}u^0(P)\|_{\overline{\omega}^h} \leq K_1, \quad (4.26)$$

where constant K_1 is independent of μ and τ . Thus, we obtain that D_2 is independent of μ and τ . Now by induction on k , we prove that all constants D_k are independent of μ , and, hence, constant $D = T \max_{1 \leq k \leq N_\tau} D_k$ in (4.15) is independent of μ and τ . Thus, we prove the theorem. \square

Remark 4.6. In the next section, we present sufficient conditions to guarantee the inequality $\tilde{r} < 1$ required in Theorem 4.5.

4.4. Uniform convergence of the monotone domain decomposition algorithm (4.1)–(4.5). Here we analyze a convergence rate of algorithm (4.1)–(4.5) applied to the difference scheme (2.5) defined on the piecewise uniform mesh (3.80).

The difference scheme (2.5) on the piecewise uniform mesh (3.80) converges μ -uniformly to the solution of (1.2):

$$\max_{t_k \in \overline{\omega}^t} \|U(t_k) - u(t_k)\|_{\overline{\omega}^h} \leq C((N^{-1} \ln N)^2 + \tau), \quad N = \min\{N_x, N_y\}, \quad (4.27)$$

where constant C is independent of μ , τ and N . The proof of this result can be found in [7].

Similar to Theorem 3.9, we have the following uniform convergence property of algorithm (4.1)–(4.5).

THEOREM 4.7. *Let the interfacial subdomains $\overline{\theta}_m^h$, $m = 1, \dots, M-1$ and $\overline{\vartheta}_l^h$, $l = 1, \dots, L-1$ be located in the x - and y -directions, respectively, outside the boundary layers (unbalanced decomposition). Suppose that $\mu \leq \mu_0 \ll 1$, and that the following conditions are satisfied*

$$\overline{N} \leq \frac{1}{\mu_0}, \quad \overline{N} = \max\{N_x, N_y\}, \quad \tau < \frac{1}{2 + c^*}. \quad (4.28)$$

If the initial upper or lower solution $V^{(0)}$ is chosen in the form of (4.14), then the monotone domain decomposition algorithm (4.1)–(4.5) on the piecewise uniform mesh (3.80) converges μ -uniformly to the solution of the problem (1.2).

Proof. Since the interfacial subdomains are located outside the boundary layers, where the step sizes h_x and h_y are in use, then under the above assumption on \overline{N} , the coefficients η and \tilde{r} in (4.15), with the notation from (4.13), satisfy the following inequalities

$$\eta \leq 2, \quad \tilde{r} = r + r^I + r^{II} \leq c^* \tau + 2\tau. \quad (4.29)$$

Thus, if $\tau < (2 + c^*)^{-1}$, as assumed in the theorem, then $\tilde{r} < 1$. From here, (4.15) and (4.27), we conclude

$$\begin{aligned} \max_{t_k \in \bar{\omega}^\tau} \|V^{(n)}(t_k) - u(t_k)\|_{\bar{\omega}^h} &\leq C((N^{-1} \ln N)^2 + \tau) + \tilde{D}(\tilde{Q})^{n_*-1}, \\ \tilde{D} &= (2 + c^*)D, \quad \tilde{Q} = (2 + c^*)\tau, \end{aligned} \quad (4.30)$$

where constants C and \tilde{D} are independent of μ , τ and N . We prove the theorem. \square

Remark 4.8. The implicit two-level difference scheme (2.5) is of first order with respect to τ . Since $\tilde{Q} = \mathcal{O}(\tau)$, one may choose $n_* = 2$ to keep the global error of algorithm (4.1)–(4.5) consistent with the global error of the difference scheme (2.5).

5. Numerical experiments

Now the monotone domain decomposition algorithms (3.5)–(3.10) and (4.1)–(4.5) are respectively applied to reaction-diffusion problems of elliptic and parabolic types. All experiments are performed on a serial computer equipped with a 2.8 GHz Pentium 4 processor. Some consequences for parallel implementation are also discussed. We consider in turn the elliptic problem

$$\begin{aligned} -\mu^2(u_{xx} + u_{yy}) + \frac{u-4}{5-u} &= 0, \quad (x, y) \in \omega = \{0 < x < 1\} \times \{0 < y < 1\}, \\ u(x, y) &= 1, \quad (x, y) \in \partial\omega, \end{aligned} \quad (5.1)$$

and its parabolic analogue

$$\begin{aligned} -\mu^2(u_{xx} + u_{yy}) + \frac{u-4}{5-u} + u_t &= 0, \quad (x, y) \in \omega, \quad t \in (0, 1], \\ u(x, y, 0) &= \begin{cases} 0, & (x, y) \in \omega, \\ 1, & (x, y) \in \partial\omega, \end{cases} \\ u(x, y, t) &= 1, \quad (x, y) \in \partial\omega, \quad t \in (0, 1]. \end{aligned} \quad (5.2)$$

The solution to the reduced elliptic problem ($\mu = 0$) is $u_r = 4$. For $\mu \ll 1$ the problem is singularly perturbed and the solution increases sharply from $u = 1$ on $\partial\omega$ to $u = 4$ on the interior. The solution to the parabolic problem approaches this steady state with time.

For the continuous problems (5.1) and (5.2), we solve the corresponding nonlinear difference schemes (2.2) and (2.5) with the monotone domain decomposition algorithms (3.5)–(3.10) and (4.1)–(4.5), respectively. We employ a piecewise uniform mesh (3.80) and suppose that $N_x = N_y = \bar{N}$. Because the mesh is only piecewise uniform, the linear system arising from the difference problem on a given subdomain may be nonsymmetric. Therefore, we solve all linear systems with the restarted GMRES algorithm from [10], suitable for nonsymmetric systems.

5.1. The elliptic problem. Define upper and lower solutions $\bar{V}^{(0)}$ and $\underline{V}^{(0)}$ by $\bar{V}^{(0)}(\omega^h) = 4$, $\bar{V}^{(0)}(\partial\omega^h) = 1$ and $\underline{V}^{(0)}(\omega^h) = 0$, $\underline{V}^{(0)}(\partial\omega^h) = 1$. We initiate the algorithm with the

Table 5.1. The parameter \tilde{q} from the convergence estimate (3.44), for balanced and unbalanced domain decomposition. The undecomposed convergence rate is $q = 0.96$.

$\bar{N} \setminus \mu$	$\tilde{q}(\text{balanced}); \tilde{q}(\text{unbalanced})$			
	10^{-1}	10^{-2}	10^{-3}	10^{-4}
2^6	83; 83	2.14; 1.56	2.1; 0.962	2.14; 0.960
2^7	329; 329	4.44; 4.05	4.44; 0.969	4.44; 0.960
2^8	1312; 1312	14.1; 14.1	11.6; 0.997	11.6; 0.960
2^9	5244; 5244	53.4; 53.4	34.6; 1.11	34.6; 0.961

lower solution $\underline{V}^{(0)}$ and it follows from Theorem 3.2 that our computed sequence satisfies $0 \leq \underline{V}^{(n)} \leq 4$. Therefore, we may consider that $f_u = 1/(5-u)^2$ is bounded above and below by $c^* = 1$ and $c_* = 1/25$, respectively. In all experiments of this section we use the convergence criterion $\|V^{(n)} - V^{(n-1)}\|_{\bar{\omega}^n} < \delta$, with $\delta = 10^{-5}$.

The undecomposed monotone iterative algorithm converges monotonically to the exact solution of (2.2) at the rate $q = 1 - c_*/c^* = 0.96$. From Theorem 3.2, the monotone domain decomposition algorithm (3.5)–(3.10) also converges monotonically to the exact solution. The decomposed convergence parameter \tilde{q} from estimate (3.44) comprises the undecomposed parameter q , augmented by two terms deriving from the decomposition in each of the x - and y -directions. If $\tilde{q} > 1$ then estimate (3.44) is of no formal use. Nevertheless, we expect that the trends in \tilde{q} with respect to μ and \bar{N} are reflected in the convergence behaviour of the algorithm. For reference, we list in Table 5.1 the value of \tilde{q} , for balanced and unbalanced domain decomposition. We mention that for $\mu = 10^{-1}$, the boundary layer thicknesses σ_x and σ_y are each 0.25 and the mesh is uniform in each direction. Hence, we do not consider unbalanced domain decomposition when $\mu = 10^{-1}$.

5.1.1. Balanced domain decomposition. We first consider balanced domain decompositions. For $\mu = 10^{-1}$, the convergence iteration counts and execution times are shown in Table 5.2. All execution times of this section have been rounded up to the nearest second. Each major cell corresponds to a certain nonlinear system (2.2) to be solved by algorithm (3.5)–(3.10). Within each major cell, results corresponding to 25 main subdomain decompositions are presented, including the undecomposed algorithm ($M = 1, L = 1$). Where there is some choice for the interfacial subdomain widths, the results corresponding to minimal and maximal choices are written above and below the line, respectively. The convergence iteration count for each undecomposed problem is 23. This increases rapidly with decomposition and mesh size \bar{N} . This reflects a value of \tilde{q} that is significantly larger than $q = 0.96$, and which increases with \bar{N} .

For $\mu \leq 10^{-2}$ we expect more reasonable iteration counts. This is demonstrated in Table 5.3. If maximal interfacial subdomain widths are chosen, the iteration count increases only slightly with decomposition. Consider now the corresponding execution times. In each of the nine major cells the execution time of the undecomposed monotone algorithm appears in the top left corner. It is interesting to note that, for each value of μ and \bar{N} , there are certain decompositions which reduce the execution time. For $\bar{N} = 2^9$ and $\mu = 10^{-2}$, the decomposition $M = 32, L = 1$ requires 90 seconds to execute if maximal interfacial subdomains are used. This is a significant reduction from the 130 seconds for

Table 5.2. Convergence iteration counts and execution times for $\mu = 10^{-1}$. Where there is some choice for the widths of the interfacial subdomains, the results corresponding to minimal and maximal interfacial subdomains are given above and below the line, respectively.

\bar{N}	2^6					2^7					2^8				
$L \setminus M$	1	4	8	16	32	1	4	8	16	32	1	4	8	16	32
	Convergence iteration count														
1	23	$\frac{133}{32}$	$\frac{212}{68}$	$\frac{374}{205}$	683	23	$\frac{241}{32}$	$\frac{387}{68}$	$\frac{688}{204}$	$\frac{1257}{681}$	23	$\frac{443}{32}$	$\frac{714}{68}$	$\frac{1269}{204}$	$\frac{2312}{681}$
4	$\frac{133}{32}$	$\frac{212}{31}$	$\frac{283}{46}$	$\frac{425}{85}$	$\frac{702}{213}$	$\frac{241}{32}$	$\frac{399}{31}$	$\frac{536}{45}$	$\frac{813}{84}$	$\frac{1346}{206}$	$\frac{443}{32}$	$\frac{746}{31}$	$\frac{1006}{45}$	$\frac{1528}{83}$	$\frac{2525}{205}$
8	$\frac{212}{68}$	$\frac{283}{46}$	$\frac{347}{68}$	$\frac{474}{120}$	$\frac{721}{241}$	$\frac{387}{68}$	$\frac{536}{46}$	$\frac{668}{68}$	$\frac{928}{117}$	$\frac{1430}{220}$	$\frac{714}{68}$	$\frac{1006}{46}$	$\frac{1260}{68}$	$\frac{1762}{117}$	$\frac{2722}{215}$
16	$\frac{374}{205}$	$\frac{425}{85}$	$\frac{474}{120}$	$\frac{570}{213}$	$\frac{757}{425}$	$\frac{688}{204}$	$\frac{813}{84}$	$\frac{928}{118}$	$\frac{1156}{206}$	$\frac{1597}{384}$	$\frac{1269}{204}$	$\frac{1528}{83}$	$\frac{1762}{117}$	$\frac{2224}{204}$	$\frac{3115}{375}$
32	683	$\frac{702}{213}$	$\frac{721}{241}$	$\frac{757}{425}$	831	$\frac{1257}{681}$	$\frac{1346}{206}$	$\frac{1430}{220}$	$\frac{1597}{384}$	$\frac{1925}{712}$	$\frac{2312}{681}$	$\frac{2525}{204}$	$\frac{2722}{215}$	$\frac{3115}{375}$	$\frac{3880}{688}$
	Execution time (s)														
1	2	$\frac{3}{2}$	$\frac{2}{2}$	$\frac{2}{2}$	1	18	$\frac{68}{18}$	$\frac{33}{11}$	$\frac{22}{12}$	$\frac{14}{12}$	421	$\frac{1807}{281}$	$\frac{1001}{222}$	$\frac{468}{139}$	$\frac{260}{140}$
4	$\frac{3}{2}$	$\frac{4}{2}$	$\frac{4}{2}$	$\frac{4}{3}$	$\frac{3}{5}$	$\frac{68}{18}$	$\frac{73}{20}$	$\frac{66}{29}$	$\frac{54}{27}$	$\frac{44}{51}$	$\frac{1805}{281}$	$\frac{1878}{303}$	$\frac{1231}{277}$	$\frac{910}{366}$	$\frac{709}{766}$
8	$\frac{2}{2}$	$\frac{4}{2}$	$\frac{3}{2}$	$\frac{3}{3}$	$\frac{3}{3}$	$\frac{33}{11}$	$\frac{66}{26}$	$\frac{52}{19}$	$\frac{46}{22}$	$\frac{40}{29}$	$\frac{1005}{222}$	$\frac{1239}{278}$	$\frac{984}{238}$	$\frac{881}{283}$	$\frac{752}{365}$
16	$\frac{2}{2}$	$\frac{3}{3}$	$\frac{3}{3}$	$\frac{2}{2}$	$\frac{3}{3}$	$\frac{22}{12}$	$\frac{55}{27}$	$\frac{46}{22}$	$\frac{32}{21}$	$\frac{32}{26}$	$\frac{465}{138}$	$\frac{921}{372}$	$\frac{880}{263}$	$\frac{663}{258}$	$\frac{595}{286}$
32	1	$\frac{3}{5}$	$\frac{3}{3}$	$\frac{3}{3}$	3	$\frac{14}{13}$	$\frac{44}{50}$	$\frac{40}{28}$	$\frac{32}{26}$	$\frac{22}{25}$	$\frac{259}{141}$	$\frac{697}{758}$	$\frac{731}{355}$	$\frac{585}{283}$	$\frac{404}{270}$

the undecomposed monotone method. For $N = 2^9$ and $\mu \leq 10^{-3}$, the domain decomposition $M = 4, L = 32$ with minimal interfacial subdomains executes fastest.

Consider a parallel implementation of algorithm (3.5)–(3.10) in which each main subdomain is wholly assigned to one of several processors in a cluster. During Step 2 of the algorithm, each of the main subdomains can be solved in serial fashion; no data transfer is necessary once the Dirichlet data have been passed. For a balanced M, L decomposition in which the number of processors divides ML , the computational cost for Step 2 of the algorithm is shared equally among the processors. During Steps 3 and 4, the idle time of those processors not assigned an interfacial subdomain will be minimized if minimal interfacial subdomains are chosen.

5.1.2. Unbalanced domain decomposition. We now consider unbalanced domain decompositions, with the interfacial subdomains located outside the boundary layers. All unbalanced domain decomposition experiments employed minimal interfacial subdomains. For $\mu \leq 10^{-2}$, convergence iteration counts are shown in Table 5.4. For $\mu = 10^{-2}$, the

Table 5.3. Iteration counts and execution times for balanced domain decompositions.

	μ	10^{-2}					10^{-3}					10^{-4}				
\bar{N}	$L \setminus M$	1	4	8	16	32	1	4	8	16	32	1	4	8	16	32
		Convergence iteration count														
2^7	1	21	$\frac{28}{21}$	$\frac{29}{21}$	$\frac{30}{22}$	$\frac{37}{27}$	21	$\frac{22}{21}$	$\frac{29}{21}$	$\frac{30}{22}$	$\frac{37}{27}$	21	$\frac{21}{21}$	$\frac{29}{21}$	$\frac{30}{22}$	$\frac{37}{27}$
	4	$\frac{28}{21}$	$\frac{28}{21}$	$\frac{29}{21}$	$\frac{30}{22}$	$\frac{38}{27}$	$\frac{22}{21}$	$\frac{22}{21}$	$\frac{29}{21}$	$\frac{30}{22}$	$\frac{37}{27}$	$\frac{21}{21}$	$\frac{21}{21}$	$\frac{29}{21}$	$\frac{30}{22}$	$\frac{37}{27}$
	8	$\frac{29}{21}$	$\frac{29}{21}$	$\frac{29}{21}$	$\frac{31}{22}$	$\frac{38}{26}$	$\frac{29}{21}$	$\frac{29}{21}$	$\frac{29}{21}$	$\frac{30}{22}$	$\frac{38}{26}$	$\frac{29}{21}$	$\frac{29}{21}$	$\frac{29}{21}$	$\frac{30}{22}$	$\frac{38}{26}$
	16	$\frac{30}{22}$	$\frac{30}{22}$	$\frac{31}{22}$	$\frac{32}{22}$	$\frac{40}{25}$	$\frac{30}{22}$	$\frac{30}{22}$	$\frac{31}{22}$	$\frac{32}{22}$	$\frac{40}{25}$	$\frac{30}{22}$	$\frac{30}{22}$	$\frac{31}{22}$	$\frac{32}{22}$	$\frac{40}{25}$
	32	$\frac{37}{27}$	$\frac{38}{27}$	$\frac{38}{26}$	$\frac{40}{25}$	$\frac{46}{27}$	$\frac{37}{27}$	$\frac{37}{27}$	$\frac{38}{26}$	$\frac{40}{25}$	$\frac{46}{27}$	$\frac{37}{27}$	$\frac{37}{27}$	$\frac{38}{26}$	$\frac{40}{25}$	$\frac{46}{27}$
2^8	1	21	$\frac{43}{21}$	$\frac{43}{21}$	$\frac{44}{22}$	$\frac{55}{26}$	21	$\frac{26}{21}$	$\frac{40}{21}$	$\frac{41}{22}$	$\frac{49}{24}$	21	$\frac{21}{21}$	$\frac{40}{21}$	$\frac{41}{22}$	$\frac{49}{24}$
	4	$\frac{43}{21}$	$\frac{46}{21}$	$\frac{46}{21}$	$\frac{48}{22}$	$\frac{62}{26}$	$\frac{26}{21}$	$\frac{26}{21}$	$\frac{40}{21}$	$\frac{41}{22}$	$\frac{49}{24}$	$\frac{21}{21}$	$\frac{21}{21}$	$\frac{40}{21}$	$\frac{41}{22}$	$\frac{49}{24}$
	8	$\frac{43}{21}$	$\frac{46}{21}$	$\frac{46}{21}$	$\frac{48}{22}$	$\frac{63}{25}$	$\frac{40}{21}$	$\frac{40}{21}$	$\frac{41}{21}$	$\frac{43}{22}$	$\frac{55}{24}$	$\frac{40}{21}$	$\frac{40}{21}$	$\frac{41}{21}$	$\frac{43}{22}$	$\frac{55}{24}$
	16	$\frac{44}{22}$	$\frac{48}{22}$	$\frac{48}{22}$	$\frac{50}{22}$	$\frac{65}{25}$	$\frac{41}{22}$	$\frac{41}{22}$	$\frac{43}{22}$	$\frac{44}{22}$	$\frac{57}{24}$	$\frac{41}{22}$	$\frac{41}{22}$	$\frac{43}{22}$	$\frac{44}{22}$	$\frac{57}{24}$
	32	$\frac{55}{26}$	$\frac{62}{26}$	$\frac{63}{25}$	$\frac{65}{25}$	$\frac{78}{25}$	$\frac{49}{24}$	$\frac{49}{24}$	$\frac{55}{24}$	$\frac{57}{24}$	$\frac{67}{24}$	$\frac{49}{24}$	$\frac{49}{24}$	$\frac{55}{24}$	$\frac{57}{24}$	$\frac{67}{24}$
2^9	1	21	$\frac{74}{21}$	$\frac{74}{21}$	$\frac{76}{22}$	$\frac{94}{25}$	21	$\frac{36}{21}$	$\frac{62}{21}$	$\frac{62}{21}$	$\frac{72}{23}$	21	$\frac{24}{21}$	$\frac{62}{21}$	$\frac{62}{21}$	$\frac{72}{23}$
	4	$\frac{74}{21}$	$\frac{89}{21}$	$\frac{89}{21}$	$\frac{92}{22}$	$\frac{116}{25}$	$\frac{36}{21}$	$\frac{36}{21}$	$\frac{62}{21}$	$\frac{62}{21}$	$\frac{72}{23}$	$\frac{24}{21}$	$\frac{24}{21}$	$\frac{62}{21}$	$\frac{62}{21}$	$\frac{72}{23}$
	8	$\frac{74}{21}$	$\frac{89}{21}$	$\frac{89}{21}$	$\frac{92}{22}$	$\frac{116}{25}$	$\frac{62}{21}$	$\frac{62}{21}$	$\frac{72}{21}$	$\frac{72}{21}$	$\frac{86}{23}$	$\frac{62}{21}$	$\frac{62}{21}$	$\frac{72}{21}$	$\frac{72}{21}$	$\frac{86}{23}$
	16	$\frac{76}{22}$	$\frac{92}{22}$	$\frac{92}{22}$	$\frac{95}{22}$	$\frac{121}{24}$	$\frac{62}{21}$	$\frac{62}{21}$	$\frac{72}{21}$	$\frac{73}{21}$	$\frac{88}{23}$	$\frac{62}{21}$	$\frac{62}{21}$	$\frac{72}{21}$	$\frac{73}{21}$	$\frac{88}{23}$
	32	$\frac{94}{25}$	$\frac{116}{25}$	$\frac{116}{25}$	$\frac{121}{24}$	$\frac{144}{25}$	$\frac{72}{23}$	$\frac{72}{23}$	$\frac{86}{23}$	$\frac{88}{23}$	$\frac{103}{23}$	$\frac{72}{23}$	$\frac{72}{23}$	$\frac{86}{23}$	$\frac{88}{23}$	$\frac{103}{23}$
		Execution time (s)														
2^7	1	2	$\frac{2}{2}$	$\frac{2}{2}$	$\frac{1}{2}$	$\frac{1}{1}$	2	$\frac{1}{2}$	$\frac{1}{2}$	$\frac{1}{2}$	$\frac{1}{1}$	2	$\frac{1}{2}$	$\frac{1}{2}$	$\frac{1}{2}$	$\frac{1}{1}$
	4	$\frac{2}{2}$	$\frac{2}{3}$	$\frac{2}{3}$	$\frac{1}{2}$	$\frac{1}{2}$	$\frac{1}{2}$	$\frac{1}{2}$	$\frac{1}{3}$	$\frac{1}{2}$	$\frac{1}{2}$	$\frac{1}{2}$	$\frac{1}{2}$	$\frac{1}{3}$	$\frac{1}{2}$	$\frac{1}{2}$
	8	$\frac{2}{2}$	$\frac{2}{3}$	$\frac{1}{2}$	$\frac{1}{2}$	$\frac{1}{2}$	$\frac{1}{2}$	$\frac{1}{2}$	$\frac{1}{2}$	$\frac{1}{2}$	$\frac{1}{2}$	$\frac{1}{2}$	$\frac{1}{3}$	$\frac{1}{2}$	$\frac{1}{2}$	$\frac{1}{2}$
	16	$\frac{1}{2}$	$\frac{1}{2}$	$\frac{1}{2}$	$\frac{1}{2}$	$\frac{1}{2}$	$\frac{1}{2}$	$\frac{1}{2}$	$\frac{1}{2}$	$\frac{1}{2}$	$\frac{1}{2}$	$\frac{1}{2}$	$\frac{1}{2}$	$\frac{1}{2}$	$\frac{1}{2}$	$\frac{1}{2}$
	32	$\frac{1}{1}$	$\frac{1}{2}$	$\frac{1}{2}$	$\frac{1}{2}$	$\frac{1}{2}$	$\frac{1}{1}$	$\frac{1}{2}$	$\frac{1}{2}$	$\frac{1}{2}$	$\frac{1}{2}$	$\frac{1}{1}$	$\frac{1}{2}$	$\frac{1}{2}$	$\frac{1}{2}$	$\frac{1}{2}$

Table 5.3. Continued.

		Execution time (s)														
2^8	1	15	$\frac{19}{17}$	$\frac{16}{16}$	$\frac{12}{13}$	$\frac{10}{9}$	13	$\frac{9}{12}$	$\frac{10}{12}$	$\frac{9}{10}$	$\frac{8}{8}$	13	$\frac{7}{12}$	$\frac{10}{12}$	$\frac{9}{10}$	$\frac{7}{8}$
	4	$\frac{19}{17}$	$\frac{17}{22}$	$\frac{14}{21}$	$\frac{13}{21}$	$\frac{13}{19}$	$\frac{9}{12}$	$\frac{6}{15}$	$\frac{7}{14}$	$\frac{6}{14}$	$\frac{5}{13}$	$\frac{7}{12}$	$\frac{5}{15}$	$\frac{7}{14}$	$\frac{5}{14}$	$\frac{5}{13}$
	8	$\frac{16}{16}$	$\frac{14}{21}$	$\frac{14}{20}$	$\frac{13}{18}$	$\frac{13}{17}$	$\frac{11}{12}$	$\frac{7}{15}$	$\frac{7}{14}$	$\frac{7}{13}$	$\frac{7}{13}$	$\frac{11}{12}$	$\frac{7}{14}$	$\frac{7}{14}$	$\frac{6}{13}$	$\frac{6}{12}$
	16	$\frac{12}{13}$	$\frac{13}{19}$	$\frac{13}{18}$	$\frac{9}{16}$	$\frac{10}{15}$	$\frac{9}{10}$	$\frac{6}{14}$	$\frac{7}{13}$	$\frac{6}{12}$	$\frac{6}{11}$	$\frac{9}{10}$	$\frac{5}{14}$	$\frac{6}{13}$	$\frac{5}{12}$	$\frac{5}{11}$
	32	$\frac{9}{9}$	$\frac{13}{18}$	$\frac{13}{17}$	$\frac{10}{15}$	$\frac{7}{11}$	$\frac{8}{9}$	$\frac{5}{13}$	$\frac{7}{13}$	$\frac{6}{12}$	$\frac{6}{10}$	$\frac{7}{8}$	$\frac{5}{13}$	$\frac{6}{12}$	$\frac{5}{11}$	$\frac{5}{10}$
2^9	1	130	$\frac{429}{251}$	$\frac{378}{231}$	$\frac{236}{144}$	$\frac{157}{90}$	95	$\frac{140}{152}$	$\frac{177}{145}$	$\frac{114}{96}$	$\frac{93}{81}$	99	$\frac{101}{153}$	$\frac{166}{145}$	$\frac{107}{95}$	$\frac{91}{79}$
	4	$\frac{429}{251}$	$\frac{303}{293}$	$\frac{271}{280}$	$\frac{234}{238}$	$\frac{196}{210}$	$\frac{142}{155}$	$\frac{65}{171}$	$\frac{89}{166}$	$\frac{72}{139}$	$\frac{57}{132}$	$\frac{100}{154}$	$\frac{44}{169}$	$\frac{81}{163}$	$\frac{64}{135}$	$\frac{44}{129}$
	8	$\frac{380}{231}$	$\frac{271}{280}$	$\frac{240}{267}$	$\frac{199}{224}$	$\frac{193}{207}$	$\frac{179}{146}$	$\frac{89}{166}$	$\frac{99}{160}$	$\frac{79}{132}$	$\frac{77}{128}$	$\frac{167}{145}$	$\frac{81}{163}$	$\frac{98}{159}$	$\frac{77}{129}$	$\frac{70}{126}$
	16	$\frac{235}{143}$	$\frac{234}{239}$	$\frac{200}{227}$	$\frac{177}{177}$	$\frac{183}{153}$	$\frac{111}{96}$	$\frac{72}{138}$	$\frac{79}{132}$	$\frac{71}{108}$	$\frac{75}{103}$	$\frac{107}{95}$	$\frac{64}{135}$	$\frac{76}{129}$	$\frac{69}{104}$	$\frac{63}{100}$
	32	$\frac{156}{91}$	$\frac{194}{209}$	$\frac{190}{208}$	$\frac{177}{152}$	$\frac{123}{117}$	$\frac{93}{78}$	$\frac{56}{133}$	$\frac{76}{130}$	$\frac{72}{105}$	$\frac{69}{89}$	$\frac{91}{79}$	$\frac{44}{130}$	$\frac{70}{128}$	$\frac{63}{101}$	$\frac{51}{86}$

results are similar to those of the corresponding balanced decomposition with minimal interfacial subdomains. This reflects similar values of \tilde{q} in Table 5.1. On the other hand, for $\mu \leq 10^{-3}$ the parameter \tilde{q} is close to the undecomposed parameter q and we observe a convergence iteration count that is independent of M and L .

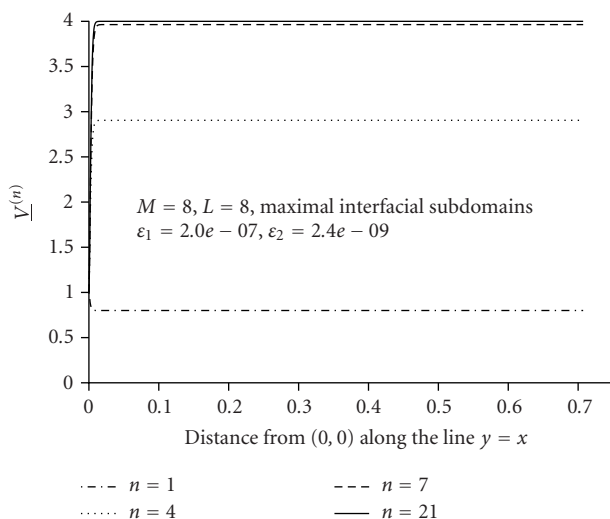
A comparison between the execution times of Table 5.4 and those of Table 5.3 shows that, for $\mu \leq 10^{-3}$, algorithm (3.5)–(3.10) executes more quickly with unbalanced domain decomposition. For a parallel implementation of algorithm (3.5)–(3.10) with unbalanced domain decomposition, load balancing at the main subdomain stage could be partially restored by solving the larger linear problems in parallel (the second level of parallelization).

5.1.3. The nature of the convergence. We expect from Theorem 3.2 that each mesh function in the sequence $\{\underline{V}^{(n)}\}$ is a lower solution to (2.2) and that the convergence at each mesh point is monotonic. On the other hand, for all numerical experiments of this paper, we solve the linear problems (3.5)–(3.8) iteratively, terminating the solution process when the system residual has decreased by order five. With this approximation, the sequence $\{\underline{V}^{(n)}\}$ violates Theorem 3.2 slightly but the effect on convergence behaviour is not catastrophic. Indeed, if one requests an order ten reduction in the system residual of each problem (3.5)–(3.8) then the computed results accord with Theorem 3.2 (to within machine accuracy).

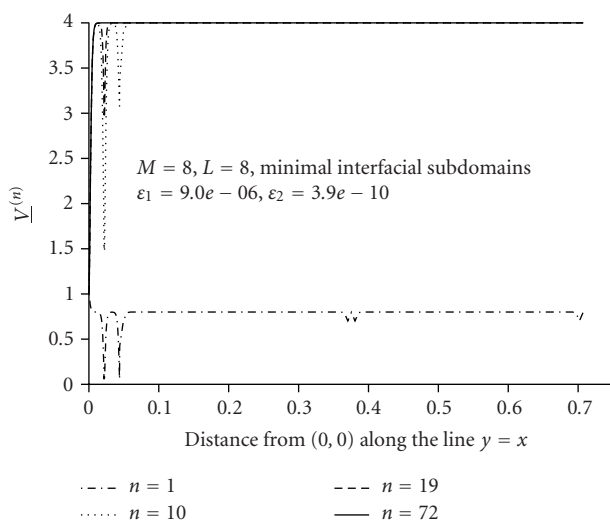
Table 5.4. Iteration counts and execution times for unbalanced domain decompositions.

	μ	10^{-2}					10^{-3}					10^{-4}				
\bar{N}	$L \setminus M$	1	4	8	16	32	1	4	8	16	32	1	4	8	16	32
		Convergence iteration count														
2^7	1	21	28	28	33	46	21	21	21	21	21	21	21	21	21	21
	4	28	28	28	33	46	21	21	21	21	21	21	21	21	21	21
	8	28	28	28	33	46	21	21	21	21	21	21	21	21	21	21
	16	33	33	33	33	46	21	21	21	21	21	21	21	21	21	21
	32	46	46	46	46	46	21	21	21	21	21	21	21	21	21	21
2^8	1	21	43	43	51	77	21	21	21	21	21	21	21	21	21	21
	4	43	46	46	52	77	21	21	21	21	21	21	21	21	21	21
	8	43	46	46	53	77	21	21	21	21	21	21	21	21	21	21
	16	51	52	53	59	77	21	21	21	21	21	21	21	21	21	21
	32	77	77	77	77	91	21	21	21	21	21	21	21	21	21	21
2^9	1	21	74	75	86	135	21	21	21	21	21	21	21	21	21	21
	4	74	89	89	99	135	21	21	21	21	21	21	21	21	21	21
	8	75	89	89	99	136	21	21	21	21	21	21	21	21	21	21
	16	86	99	99	110	148	21	21	21	21	21	21	21	21	21	21
	32	135	135	136	148	184	21	21	21	21	21	21	21	21	21	21
		Execution time (s)														
2^7	1	2	2	2	2	2	2	1	1	1	1	2	1	1	1	1
	4	2	2	2	2	2	1	1	1	1	1	1	1	1	1	1
	8	2	2	1	1	2	1	1	1	1	1	1	1	1	1	1
	16	2	2	1	1	2	1	1	1	1	1	1	1	1	1	1
	32	2	2	2	2	1	1	1	1	1	1	1	1	1	1	1
2^8	1	15	19	16	16	20	13	7	7	7	7	13	7	7	7	7
	4	18	16	15	15	19	8	5	5	5	5	7	5	5	5	5
	8	16	15	14	14	17	7	5	5	5	5	7	5	4	5	5
	16	16	15	14	13	15	7	5	5	5	5	7	5	5	5	5
	32	20	19	17	15	15	7	5	5	5	5	7	5	5	5	5
2^9	1	130	432	375	336	445	101	89	82	75	72	100	89	82	74	72
	4	431	309	276	264	307	89	41	39	38	38	89	41	40	38	38
	8	374	278	249	242	284	82	39	37	36	36	82	39	37	36	36
	16	335	263	241	226	260	74	38	36	35	35	75	38	36	35	35
	32	444	306	283	260	275	72	38	36	35	35	72	38	36	35	35

In Figure 5.1 we show the convergence behaviour of algorithm (3.5)–(3.10) for the problem with $\mu = 10^{-3}$ and $\bar{N} = 512$. The first graph corresponds to the balanced decomposition with $M = 8$, $L = 8$ and maximal interfacial subdomains while the second graph corresponds to the balanced decomposition with $M = 8$, $L = 8$ and minimal interfacial



(a)



(b)

Figure 5.1. Profiles of $\underline{V}^{(n)}$ for various iteration numbers n and two different balanced domain decompositions. The problem has $\mu = 10^{-3}$ and $\bar{N} = 512$.

subdomains. Also indicated in each graph is the degree to which the computed iterates violate Theorem 3.2. We define ϵ_1 as the maximum difference scheme residual

$$\epsilon_1 = \max \{ \mathcal{L}^h \underline{V}^{(n)}(P) + f(P, \underline{V}^{(n)}(P)) : P \in \omega^h, n = 0, 1, \dots \}, \quad (5.3)$$

while ϵ_2 measures the nonmonotonicity between successive iterates

$$\epsilon_2 = | \min \{ \underline{V}^{(n)}(P) - \underline{V}^{(n-1)}(P) : P \in \bar{\omega}^h, n = 1, 2, \dots \} |. \quad (5.4)$$

As mentioned above, one can reduce ϵ_1 and ϵ_2 to the order of machine accuracy by solving the linear problems (3.5)–(3.8) with sufficient accuracy.

With maximal interfacial subdomains, each iterate exhibits a smooth profile. With minimal interfacial subdomains on the other hand, each early iterate oscillates in the vicinity of the main subdomain interfaces, particularly inside the boundary layers. Although the iterates reach the interior value of 4 just as quickly as for maximal interfacial subdomains, further iterations are required to smooth the oscillation in the boundary layer. It is interesting to observe that, in spite of the oscillatory nature of each iterate, the convergence of the sequence at each mesh point is monotonic to within $\epsilon_2 = 3.9 \times 10^{-10}$.

Finally, we explain the relatively rapid convergence of the algorithm on unbalanced decompositions. Although the interfacial subdomains are minimal, they are located wholly outside the boundary layers. Therefore, the oscillation at each interface is quite small and eliminated after only a few iterations.

5.2. The parabolic problem. The numerical solution at $t = 0$ is given by the initial condition; $V(\omega^h, 0) = 0$, $V(\partial\omega^h, 0) = 1$. If we define $\underline{V}^{(0)}(\bar{\omega}^h, t_1) = V(\bar{\omega}^h, 0)$ then $\underline{V}^{(0)}(P, t_1)$ is clearly a lower solution with respect to $V(P, 0)$. We initiate the algorithm with $\underline{V}^{(0)}(P, t_1)$ and thus generate a sequence of mesh functions $\{\underline{V}^{(n)}(P, t_1)\}$ that are each lower solutions with respect to $V(P, 0)$. Consider also the mesh function $\bar{V}^{(0)}(P, t_1)$, defined by $\bar{V}^{(0)}(\omega^h, t_1) = 4$, $\bar{V}^{(0)}(\partial\omega^h, t_1) = 1$. Since $\bar{V}^{(0)}(P, t_1)$ is an upper solution with respect to $V(P, 0)$, it follows from Theorem 3.2 that $0 \leq \underline{V}^{(n)}(P, t_1) \leq 4$, $P \in \bar{\omega}^h$, $n \geq 0$. Now for $k \geq 2$, let $V(P, t_{k-1}) = \underline{V}^{(n_*)}(P, t_{k-1})$ with n_* minimal subject to

$$\| \underline{V}^{(n_*)}(t_{k-1}) - \underline{V}^{(n_*-1)}(t_{k-1}) \|_{\bar{\omega}^h} < \delta, \quad (5.5)$$

where the specified tolerance δ throughout this section is 10^{-5} . Since the boundary condition g and the function f in (5.2) are independent of time, the mesh functions $\underline{V}^{(0)}(P, t_k)$, $\bar{V}^{(0)}(P, t_k)$ defined by $\underline{V}^{(0)}(P, t_k) = V(P, t_{k-1})$, $\bar{V}^{(0)}(P, t_k) = \bar{V}^{(0)}(P, t_1)$ are respectively lower and upper solutions with respect to $V(P, t_{k-1})$. Applying Theorem 3.2, one has by induction on k that

$$0 \leq \underline{V}^{(n)}(P, t_k) \leq 4, \quad P \in \bar{\omega}^h, \quad 0 \leq n \leq n_*, \quad 0 \leq k \leq N_\tau. \quad (5.6)$$

Since each of our computed mesh functions satisfies the above inequalities, we may suppose that f_u is bounded above and below by $c^* = 1$ and $c_* = 1/25$, respectively.

At each time step t_k , the undecomposed monotone iterative algorithm with $M = 1$ and $L = 1$ converges monotonically to the exact solution $U(P, t_k)$ of (2.5). The convergence rate is $r = c^*/(c^* + \tau^{-1})$. From Theorem 4.5, algorithm (4.1)–(4.5) also converges monotonically to $U(P, t_k)$. The convergence parameter \tilde{r} from estimate (4.13) comprises the undecomposed parameter r , augmented by terms arising from each of the x - and y -decompositions. The values of \tilde{r} are listed in Table 5.5 for balanced and unbalanced domain decomposition. Throughout this section, we take as our time step $\tau = 0.1$. Similar

Table 5.5. The parameter \tilde{r} from the convergence estimate (4.13), for balanced and unbalanced domain decomposition. The time step is $\tau = 0.1$ and the undecomposed parameter r is 0.091.

$\overline{N} \setminus \mu$	$\tilde{r}(\text{balanced}); \tilde{r}(\text{unbalanced})$			
	10^{-1}	10^{-2}	10^{-3}	10^{-4}
2^6	7.54; 7.54	0.199; 0.145	0.199; 0.091	0.199; 0.091
2^7	29.9; 29.9	0.407; 0.372	0.407; 0.092	0.407; 0.091
2^8	119; 119	1.28; 1.28	1.06; 0.094	1.06; 0.091
2^9	477; 477	4.86; 4.86	3.15; 0.104	3.15; 0.091

Table 5.6. Average convergence iteration counts for simulations of ten time steps, with $\mu = 10^{-1}$.

\overline{N}	2^6					2^7					2^8				
	$L \setminus M$	1	4	8	16	32	1	4	8	16	32	1	4	8	16
1	5.0	<u>16.0</u>	<u>17.0</u>	<u>21.7</u>	<u>35.2</u>	5.0	<u>30.1</u>	<u>31.3</u>	<u>39.0</u>	<u>61.3</u>	5.0	<u>55.8</u>	<u>57.8</u>	<u>71.3</u>	<u>109.9</u>
		5.1	7.0	13.0			5.1	7.0	13.0	34.6		5.1	7.0	13.0	34.5
4	<u>16.0</u>	<u>20.6</u>	<u>21.5</u>	<u>25.7</u>	<u>36.5</u>	<u>30.1</u>	<u>40.1</u>	<u>42.0</u>	<u>49.4</u>	<u>68.5</u>	<u>55.8</u>	<u>77.7</u>	<u>80.9</u>	<u>94.1</u>	<u>128.6</u>
		5.1	5.2	6.4	11.4	29.1	5.1	5.1	6.3	11.3	28.5	5.1	5.1	6.3	11.2
8	<u>17.0</u>	<u>21.6</u>	<u>22.7</u>	<u>26.7</u>	<u>37.2</u>	<u>31.3</u>	<u>42.0</u>	<u>43.8</u>	<u>51.5</u>	<u>70.4</u>	<u>57.8</u>	<u>80.9</u>	<u>83.9</u>	<u>97.7</u>	<u>132.4</u>
		7.0	6.4	7.0	10.1	22.5	7.0	6.3	7.0	10.0	21.5	7.0	6.3	7.0	10.0
16	<u>21.7</u>	<u>25.7</u>	<u>26.7</u>	<u>30.3</u>	<u>38.7</u>	<u>39.0</u>	<u>49.4</u>	<u>51.5</u>	<u>59.0</u>	<u>76.7</u>	<u>71.3</u>	<u>94.1</u>	<u>97.7</u>	<u>112.3</u>	<u>146.0</u>
		13.0	11.3	10.1	13.8	24.9	13.0	11.2	10.0	13.0	22.3	13.0	11.2	10.0	13.0
32	<u>35.2</u>	<u>36.6</u>	<u>37.2</u>	<u>38.7</u>	<u>42.4</u>	<u>61.3</u>	<u>68.5</u>	<u>70.5</u>	<u>76.8</u>	<u>90.4</u>	<u>109.9</u>	<u>128.6</u>	<u>132.4</u>	<u>146.0</u>	<u>176.0</u>
		29.1	22.3	24.7			34.6	28.3	21.3	22.2	36.3	34.5	28.2	20.9	22.0

to the elliptic problem, we expect that the values of \tilde{r} will be reflected in the convergence behaviour of algorithm (4.1)–(4.5).

5.2.1. *Balanced domain decomposition.* Shown in Table 5.6 are average convergence iteration counts for $\mu = 10^{-1}$. The average is taken over the first ten time steps. The large values of \tilde{r} are reflected in the algorithm’s convergence behaviour under domain decomposition.

For $\mu \leq 10^{-2}$, the average convergence iteration counts are shown in Table 5.7. For $\overline{N} = 2^6$, \tilde{r} exceeds r by a factor of approximately two. Thus the iteration count increases slightly with decomposition. For $\overline{N} \geq 2^7$, \tilde{r} exceeds r by a factor of at least four and, for minimal interfacial subdomains, the increase in iteration count with decomposition is more marked. For $\overline{N} \geq 2^8$ it is interesting to note that, in contrast to the results for $\overline{N} = 2^7$, the iteration count is independent of decomposition if maximal interfacial subdomains are employed. Nevertheless, the execution times of Table 5.7 demonstrate that for almost all balanced domain decompositions, algorithm (4.1)–(4.5) executes more quickly when minimal interfacial subdomains are used. Consider now the results for $\overline{N} = 2^9$. For $\mu = 10^{-2}$, the undecomposed monotone algorithm executes fastest while for $\mu \leq 10^{-3}$, there are certain decompositions under which algorithm (4.1)–(4.5) executes more quickly than the undecomposed algorithm.

Table 5.7. Continued.

		Execution time (s)														
2^8	1	7	$\frac{10}{10}$	$\frac{9}{10}$	$\frac{7}{8}$	$\frac{6}{7}$	9	$\frac{6}{9}$	$\frac{7}{8}$	$\frac{6}{7}$	$\frac{6}{6}$	8	$\frac{6}{8}$	$\frac{7}{8}$	$\frac{6}{7}$	$\frac{5}{6}$
	4	$\frac{10}{10}$	$\frac{10}{13}$	$\frac{9}{14}$	$\frac{9}{13}$	$\frac{8}{12}$	6	$\frac{4}{9}$	$\frac{5}{10}$	$\frac{5}{10}$	$\frac{5}{9}$	$\frac{6}{8}$	$\frac{4}{10}$	$\frac{4}{10}$	$\frac{4}{9}$	$\frac{4}{8}$
	8	$\frac{9}{10}$	$\frac{9}{13}$	$\frac{9}{14}$	$\frac{9}{13}$	$\frac{8}{12}$	7	$\frac{5}{8}$	$\frac{6}{10}$	$\frac{6}{10}$	$\frac{5}{9}$	$\frac{7}{8}$	$\frac{4}{10}$	$\frac{5}{10}$	$\frac{5}{9}$	$\frac{5}{8}$
	16	$\frac{7}{8}$	$\frac{9}{13}$	$\frac{9}{14}$	$\frac{10}{13}$	$\frac{8}{12}$	6	$\frac{5}{8}$	$\frac{6}{10}$	$\frac{6}{10}$	$\frac{5}{9}$	$\frac{6}{8}$	$\frac{4}{10}$	$\frac{5}{10}$	$\frac{5}{9}$	$\frac{5}{8}$
	32	$\frac{6}{6}$	$\frac{8}{11}$	$\frac{8}{12}$	$\frac{8}{11}$	$\frac{6}{10}$	5	$\frac{4}{9}$	$\frac{5}{9}$	$\frac{5}{9}$	$\frac{5}{8}$	$\frac{5}{6}$	$\frac{4}{9}$	$\frac{5}{9}$	$\frac{5}{8}$	$\frac{4}{7}$
2^9	1	60	$\frac{220}{147}$	$\frac{196}{142}$	$\frac{131}{96}$	$\frac{92}{74}$	67	$\frac{84}{101}$	$\frac{110}{98}$	$\frac{76}{69}$	$\frac{63}{59}$	66	$\frac{72}{103}$	$\frac{110}{97}$	$\frac{78}{75}$	$\frac{63}{59}$
	4	$\frac{221}{147}$	$\frac{176}{184}$	$\frac{160}{181}$	$\frac{141}{158}$	$\frac{118}{146}$	84	$\frac{41}{101}$	$\frac{57}{113}$	$\frac{51}{99}$	$\frac{39}{89}$	73	$\frac{35}{104}$	$\frac{53}{117}$	$\frac{48}{101}$	$\frac{36}{92}$
	8	$\frac{196}{142}$	$\frac{159}{182}$	$\frac{142}{181}$	$\frac{123}{156}$	$\frac{115}{145}$	110	$\frac{57}{98}$	$\frac{61}{99}$	$\frac{54}{101}$	$\frac{49}{92}$	110	$\frac{53}{98}$	$\frac{61}{116}$	$\frac{53}{100}$	$\frac{47}{91}$
	16	$\frac{130}{96}$	$\frac{140}{156}$	$\frac{125}{155}$	$\frac{126}{132}$	$\frac{114}{125}$	74	$\frac{51}{69}$	$\frac{54}{98}$	$\frac{53}{86}$	$\frac{49}{79}$	75	$\frac{47}{69}$	$\frac{53}{101}$	$\frac{52}{99}$	$\frac{46}{86}$
	32	$\frac{91}{74}$	$\frac{116}{143}$	$\frac{115}{145}$	$\frac{113}{123}$	$\frac{97}{109}$	62	$\frac{38}{89}$	$\frac{47}{93}$	$\frac{48}{79}$	$\frac{44}{72}$	62	$\frac{35}{58}$	$\frac{46}{92}$	$\frac{46}{78}$	$\frac{40}{71}$

5.2.2. *Unbalanced domain decomposition.* Average convergence iteration counts for unbalanced domain decomposition are shown in Table 5.8. For $\mu \leq 10^{-3}$, \tilde{r} is sufficiently close to r and the convergence is independent of M and L . The corresponding execution times are shown in Table 5.8. As with the elliptic problem, for $\mu \leq 10^{-3}$ the algorithm executes more quickly when the domain decomposition is unbalanced.

5.2.3. *The nature of the convergence.* For all experiments of this paper, on each time step t_k , Theorem 4.1 holds true to within machine accuracy. That is, each mesh function of the sequence $\{\underline{V}^{(n)}(P, t_k)\}$ is a lower solution with respect to $V(t_{k-1})$ and the convergence of $\{\underline{V}^{(n)}(P, t_k)\}$ is monotonic at each mesh point $P \in \bar{\omega}^h$. In Figure 5.2 we show the boundary layer profile at four different times. At $t = 0.6$ the boundary layer has developed a parabolic profile. (The steady state for this problem is reached at approximately $t = 12$, beyond our considered range.)

5.3. **Discussion.** We draw the following conclusions with regard to each of the monotone domain decomposition algorithms (3.5)–(3.10) and (4.1)–(4.5).

- (i) For all values of μ and \bar{N} , and all domain decompositions, the convergence to the exact solution of the nonlinear difference scheme is monotonic.
- (ii) The convergence iteration count reflects the corresponding convergence parameter \tilde{q} or \tilde{r} from (3.44) or (4.13), respectively.
- (iii) When the decomposed convergence parameter \tilde{q} (or \tilde{r}) is sufficiently close to the undecomposed convergence parameter q (or r), the convergence rate is independent of M and L . This is observed for $\mu \leq 10^{-3}$ with unbalanced domain decomposition.

Table 5.8. Average convergence iteration counts and total execution times for simulations of ten time steps with unbalanced domain decompositions.

	μ	10^{-2}					10^{-3}					10^{-4}				
\bar{N}	$L \setminus M$	1	4	8	16	32	1	4	8	16	32	1	4	8	16	32
		Convergence iteration count														
2^7	1	5.0	6.0	6.0	6.0	7.0	5.0	5.0	5.0	5.0	5.0	5.0	5.0	5.0	5.0	5.0
	4	6.0	6.0	6.0	6.0	7.0	5.0	5.0	5.0	5.0	5.0	5.0	5.0	5.0	5.0	5.0
	8	6.0	6.0	6.0	6.0	7.0	5.0	5.0	5.0	5.0	5.0	5.0	5.0	5.0	5.0	5.0
	16	6.0	6.0	6.0	6.0	7.0	5.0	5.0	5.0	5.0	5.0	5.0	5.0	5.0	5.0	5.0
	32	7.0	7.0	7.0	7.0	7.0	5.0	5.0	5.0	5.0	5.0	5.0	5.0	5.0	5.0	5.0
2^8	1	5.0	8.0	8.0	8.0	8.0	5.0	5.0	5.0	5.0	5.0	5.0	5.0	5.0	5.0	5.0
	4	8.0	9.0	9.0	9.0	9.0	5.0	5.0	5.0	5.0	5.0	5.0	5.0	5.0	5.0	5.0
	8	8.0	9.0	9.0	9.0	9.0	5.0	5.0	5.0	5.0	5.0	5.0	5.0	5.0	5.0	5.0
	16	8.0	9.0	9.0	9.0	9.0	5.0	5.0	5.0	5.0	5.0	5.0	5.0	5.0	5.0	5.0
	32	8.0	9.0	9.0	9.2	10.0	5.0	5.0	5.0	5.0	5.0	5.0	5.0	5.0	5.0	5.0
2^9	1	5.0	13.0	13.0	13.0	13.3	5.0	5.0	5.0	5.0	5.0	5.0	5.0	5.0	5.0	5.0
	4	13.0	16.0	16.0	16.0	17.0	5.0	5.0	5.0	5.0	5.0	5.0	5.0	5.0	5.0	5.0
	8	13.0	16.0	16.0	16.0	17.0	5.0	5.0	5.0	5.0	5.0	5.0	5.0	5.0	5.0	5.0
	16	13.0	16.0	16.0	16.0	17.0	5.0	5.0	5.0	5.0	5.0	5.0	5.0	5.0	5.0	5.0
	32	13.3	17.0	17.0	17.0	17.0	5.0	5.0	5.0	5.0	5.0	5.0	5.0	5.0	5.0	5.0
		Execution time (s)														
2^7	1	1	1	1	1	1	1	1	1	1	1	1	1	1	1	1
	4	1	1	1	1	1	1	1	1	1	1	1	1	1	1	1
	8	1	1	1	1	1	1	1	1	1	1	1	1	1	1	1
	16	1	1	1	1	1	1	1	1	1	1	1	1	1	1	1
	32	1	1	1	1	1	1	1	1	1	1	1	1	1	1	1
2^8	1	7	10	9	8	7	9	5	5	5	5	9	6	5	5	5
	4	10	10	9	9	8	5	4	4	4	4	5	4	4	4	4
	8	9	9	9	9	8	5	4	4	4	4	5	4	4	4	4
	16	8	9	9	8	8	5	4	4	4	4	5	4	4	4	4
	32	7	8	8	8	8	5	4	4	4	4	5	4	4	4	4
2^9	1	60	221	198	158	145	67	61	56	53	51	67	61	57	53	51
	4	221	178	162	150	150	61	30	29	28	29	61	31	29	28	28
	8	197	162	149	141	141	60	28	28	26	27	56	29	28	27	27
	16	158	150	140	131	129	52	28	26	26	26	52	28	27	26	26
	32	144	149	140	129	116	50	28	26	26	26	50	28	27	26	26

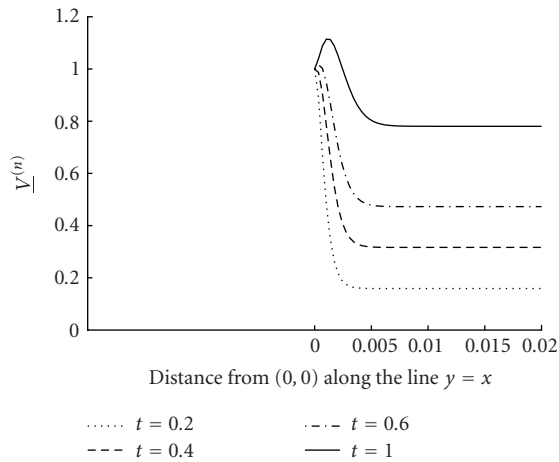


Figure 5.2. The boundary layer profile as a function of time for the problem with $\mu = 10^{-3}$ and $\bar{N} = 512$. The domain decomposition is balanced with $M = 8$, $L = 8$ and minimal interfacial subdomains.

- (iv) For $\mu \leq 10^{-3}$, the convergence iteration count is uniform with respect to μ .
- (v) For $\mu \leq 10^{-3}$, there are certain domain decompositions under which the algorithm executes more quickly than the undecomposed algorithm.
- (vi) For $\mu \leq 10^{-3}$, the algorithm executes more quickly when the domain decomposition is unbalanced rather than balanced.

References

- [1] I. Boglaev, *A numerical method for a quasilinear singular perturbation problem of elliptic type*, USSR Computational Mathematics and Mathematical Physics **28** (1988), 492–502.
- [2] ———, *Numerical solution of a quasilinear parabolic equation with a boundary layer*, USSR Computational Mathematics and Mathematical Physics **30** (1990), no. 3, 55–63.
- [3] ———, *Monotone iterative algorithms for a nonlinear singularly perturbed parabolic problem*, Journal of Computational and Applied Mathematics **172** (2004), no. 2, 313–335.
- [4] ———, *On monotone iterative methods for a nonlinear singularly perturbed reaction-diffusion problem*, Journal of Computational and Applied Mathematics **162** (2004), no. 2, 445–466.
- [5] O. A. Ladyženskaja, V. A. Solonnikov, and N. N. Ural'ceva, *Linear and Quasilinear Equations of Parabolic Type*, Translations of Mathematical Monographs, vol. 23, Izdat. “Nauka”, Moscow, 1968.
- [6] O. A. Ladyženskaja and N. N. Ural'ceva, *Linear and Quasi-Linear Elliptic Equations*, Academic Press, New York, 1968.
- [7] J. J. H. Miller, E. O’Riordan, and G. I. Shishkin, *Fitted Numerical Methods for Singular Perturbation Problems*, World Scientific, New Jersey, 1996.
- [8] C. V. Pao, *Monotone iterative methods for finite difference system of reaction-diffusion equations*, Numerische Mathematik **46** (1985), no. 4, 571–586.
- [9] ———, *Finite difference reaction diffusion equations with nonlinear boundary conditions*, Numerical Methods for Partial Differential Equations. An International Journal **11** (1995), no. 4, 355–374.

- [10] Y. Saad and M. H. Schultz, *GMRES: a generalized minimal residual algorithm for solving non-symmetric linear systems*, SIAM Journal on Scientific and Statistical Computing 7 (1986), no. 3, 856–869.
- [11] A. A. Samarskii, *The Theory of Difference Schemes*, Monographs and Textbooks in Pure and Applied Mathematics, vol. 240, Marcel Dekker, New York, 2001.

Igor Boglaev: Institute of Fundamental Sciences, Massey University, Private Bag 11-222,
Palmerston North, New Zealand
E-mail address: i.boglaev@massey.ac.nz

Matthew Hardy: Institute of Fundamental Sciences, Massey University, Private Bag 11-222,
Palmerston North, New Zealand
E-mail address: m.p.hardy@massey.ac.nz